Removal of Hexavalent Chromium from Groundwater

Using Stannous Chloride Reductive Treatment

by

Duong Thanh Nguyen

A Thesis Presented in Partial Fulfillment
of the Requirements for the Degree
Master of Science

Approved December 2018 by the
Graduate Supervisory Committee:

Paul Westerhoff, Chair
Shahnawaz Sinha
Anca Delgado

ARIZONA STATE UNIVERSITY

May 2019

ABSTRACT

Mineral weathering and industrial activities cause elevated concentration of hexavalent chromium (Cr(VI)) in groundwater, and this poses potential health concern (>10 ppb) to southwestern USA. The conversion of Cr(VI) to Cr(III) – a fairly soluble and non-toxic form at typical pH of groundwater is an effective method to control the mobility and carcinogenic effects of Cr(VI). In-situ chemical reduction using $SnCl_2$ was investigated to initiate this redox process using jar testing with buffered ultrapure water and native Arizona groundwater spiked with varying Cr(VI) concentrations. Cr(VI) transformation by $SnCl_2$ is super rapid (<60 seconds) and depends upon the molar dosage of Sn(II) to Cr(VI). Cr(VI) removal improved significantly at higher pH while was independent on Cr(VI) initial concentration and dissolved oxygen (DO) level. Co-existing oxyanions (As and W) competed with Cr(VI) for $SnCl_2$ oxidation and adsorption sites of formed precipitates, thus resulted in lower Cr(VI) removal in the challenge water. $SnCl_2$ reagent grade and commercial grade behaved similarly when freshly prepared, but the reducing strength of the commercial product decreased by 50% over a week after exposing to atmosphere. Equilibrium modeling with Visual MINTEQ suggested redox potential < 400 mV to reach Cr(VI) treatment goal of 10 ppb. Kinetics of Cr(VI) reduction was simulated via the rate expression: $r=-k[H^+]^{-0.25}[Sn^{2+}]^{0.5}[Cr_2O_7^{2-}]^3$ with k = 0.146 $uM^{-2.25}s^{-1}$, which correlated consistently with experimental data under different pH and $SnCl_2$ doses. These results proved $SnCl_2$ reductive treatment is a simple and highly effective method to treat Cr(VI) in groundwater.

DEDICATION

To my parents: Hai T. Nguyen, Hai V. Nguyen, my fiancée: Phuong Trinh,

and my younger sister: Anh Nguyen for their endless love and tremendous support

in every chapter of my life.

ACKNOWLEDGEMENT

TABLE OF CONTENTS

LIST OF TABLES

LIST OF FIGURES

CHAPTER 1. INTRODUCTION

1.1. Background

Chromium (Cr) is a redox-active element exists in soil and groundwater with two stable oxidation states of (+6) and (+3) (Joe-Wong et al. 2017). While Cr(III) is an essential micronutrient for glucose metabolism and amino acid synthesis, Cr(VI) has been classified as a carcinogenic agent (Ball et al. 2004, Sedman 2006). Despite its high toxicity and mobility in subsurface environment, Cr(VI) is not currently controlled by US Environmental Protection Agency. However, total chromium (Cr(VI) + Cr(III)) is regulated with a maximum contamination level (MCL) of 100 µg/L (Li et al. 2016). Recently, State of California initially established a health advisory level for Cr(VI) at 10 µg/L in 2014 but Sacramento County Superior Court invalidated this regulation because of the failure to comply with economic feasibility in 2016 (California Department of Public Health 2016). If nationwide regulations for Cr(VI) are developed in the future, there will be a huge demand for mitigation technologies to remove Cr(VI) from groundwater.

Redox chemistry of chromium provides insights into its fate and behavior in natural water. In groundwater (pH = 6-8.5), Cr(VI) prevalently found as CrO_4^{2-} and Cr(III) typically forms hydroxide complexes as $Cr(OH)_3^0$, $Cr(OH)_2^+$, $Cr(OH)_4^-$ (Langlois et al. 2015). Solid $Cr(OH)_3$ forms at >20 µg/L concentration at pH=7-10, dehydrates and crystallizes as Cr_2O_3 at equilibrium (Rai et al. 1987).

Cr(VI) predominates at highly aerobic condition and Cr(III) is the dominant species in low/no oxygenated drinking water (McNeill et al. 2012).. Aquatic chemistry of chromium can be exploited for various treatment options such as: (1): low solubility of Cr(III) at pH >=7 suggested precipitation method; (2) the complexation of chromium with molecular

compounds proposed precipitation, sedimentation, and filtration methods; (3) high redox potential of hazardous Cr(VI) encouraged in-situ chemical reduction to transform to innocuous Cr(III); (4): electrostatic attraction of Cr(VI) oxyanion to positively charged surface recommended sorption or ion-exchange processes (Bowen et al. 2014).

Hexavalent chromium can be removed from groundwater to <5 ppb by four main physicochemical methods: reduction-coagulation-filtration (RCF), strong-base anion exchange (SBA-IX), weak-base anion exchange (WBA-IX), and reverse osmosis (RO) (Bowen et al. 2014). Nevertheless, several limitations regarding cost-effectiveness, disposal, and upscaling are needed to confront. SBA-IX generates waste brines with high concentration of Cr(VI) whereas WBA-IX works effectively only at low pH condition (Blute and Wu 2012, McGuire et al. 2006). RO operates with a low water recovery and requires costly waste disposal (Yoon et al. 2009, Plummer et al. 2018). RCF was proved to be feasible at bench- and pilot-scale, applies three major groups of chemical reductants: iron-based chemicals (zero-valent iron, ferrous sulfate, carbonate green rust, etc.), sulfur compounds (sodium sulfite, calcium polysulfide, mackinawite, etc.), and organic matter (gallic, ascorbic, and oxalic acids, etc.) (Lai et al. 2008, Qin et al. 2005, William et al. 2001, Pettine et al. 2006, Wazne et al. 2007, Mullet et al. 2004, Chen et al. 2015, Xu et al. 2004, K. Worbel et al. 2015).

RCF system with $FeSO_4$ exhibited high removal efficiency and reasonable cost application. (Lee and Hering 2003, Brandhuber et al. 2004, Qin et al. 2005). For 100 µg/L Cr(VI), <5 mg/L Fe(II) is adequate to achieve a satisfactory effluent Cr(VI) of <10 µg/L within 5

minutes. Alternatively, stannous chloride ($SnCl_2$) – a corrosion inhibitor used in water treatment plants may be capable to convert Cr(VI) to Cr(III).

RCF system with $SnCl_2$ shows remarkable advantages compared to with $FeSO_4$. Firstly, $FeSO_4$ system required Fe(II) oxidation to Fe(III) by oxidants or oxygenation because dissolved Fe(II) is controlled under US EPA secondary MCL of 300 µg/L for Fe. Secondly, $SnCl_2$ is not listed as a potential contaminant for drinking water since 2017 UL certified for Sn to meet NSF/ANSI 61 of 0.63 mg/L was removed (Kaprara et al. 2017). Thirdly, RCF with $FeSO_4$ generated a larger amount of sludge than with $SnCl_2$ which requires dewatering, disposal, and further treatment.

$SnCl_2$ application to water treatment has been reported to (1): synthesizing $SnO_2/Sn(OH)_2$ adsorbents (Rivas and Aguirre 2010), (2): producing $Sn_6O_4(OH)_4$ adsorbents/reductants (Pinakidou et al. 2016, Kaprara et al. 2017), (3): reducing Hg(II) to Hg(0) (Matthews et al. 2015, Looney et al. 2003). Brandhuber et al. 2004 and Lai and McNeill. 2006 applied 1300 µg/L Sn(II) to remove 100 µg/L Cr(VI) from groundwater at pH = 5,7,9. Cr(VI) was removed by 60% within 30 minutes, however, 0.45 µm-filtered samples showed an unusual higher Cr(VI) level than non-filtered samples. Kennedy et al. 2018 investigated the filterability of Cr(T) after reduction with pleated cartridge filter, depth cartridge filter, and sand filter in a pilot-scale system.

1.2. Organization of the thesis

The knowledge gaps from previous studies on (1): Cr(VI) removal performance using various $SnCl_2$ dosages, (2): Effects of water chemistry to Cr(VI) removal and (3): Kinetics

and speciation during Cr(VI) reduction encouraged us to examine further $SnCl_2$ reductive treatment. This thesis aims to determine the optimal $SnCl_2$ dose for Cr(VI) removal and elucidate the effects of pH, initial Cr(VI) concentration, dissolved oxygen level, and co-existing oxyanions (As and W) to Cr(VI) reduction kinetics. Furthermore, Cr(VI) reduction capacity was compared between different $SnCl_2$ source (reagent grade vs commercial grade) and water matrix (buffered water and real Arizona groundwater) to figure out the best operations for $SnCl_2$ treatment unit. Thermodynamic and kinetic models were extensively developed to understand Cr and Sn equilibrium speciation, predict the associated mineral phases, and quantify the extent and timescale of Cr(VI) reduction. These understandings are critical to implement this novel treatment technology to different water settings in SRP service area.

The thesis is organized into the following chapters with specific objectives as below:

Chapter 2: Describe experimental, analytical, and modeling methods

Chapter 3: Investigate effects of water chemistries and settings to the kinetics of Cr(VI) reduction. Develop thermodynamic and kinetic models for Cr-Sn transformation.

Chapter 4. Summarize the results, draw conclusions, and give recommendations for Salt River Project. Propose the areas for future investigations.

CHAPTER 2. MATERIALS AND METHODS

2.1. Materials

All chemicals were reagent grade except $SnCl_2$ commercial product. Ultrapure water (>18 MΩ-cm) was used for all experiments. $K_2Cr_2O_7$ (Sigma-Aldrich (ACS), > 99%) was used as the source of Cr(VI) and the tested waters were prepared by spiking 50 µg/L Cr(VI) into: buffered water with 5 mM $NaHCO_3$ (Fisher Scientific (ACS), >99%) and groundwater collected from local source in Scottsdale, AZ.

Sn(II) dosages of 0, 88.5, 177, 265, 620, 885, 1770 µg/L were prepared from 50 mM $SnCl_2$ stock solution (Sigma-Aldrich (ACS), >99.99%). Commercial source of $SnCl_2$ (PAS-8150) was from Guard Product - a NSF approved vendor for drinking water treatment (Pleasanton, CA). PAS-8150 samples were procured twice on 11/2/2017 and 7/14/2018 as 50% $SnCl_2$ opened solution and diluted before testing.

0.1 M NaOH and 0.1 M HCl were used before reduction experiment to adjust pH and 0.025 M NaCl was used to maintain a constant ionic strength for these waters.

2.2. Reduction Experiments

Cr(VI) reduction by $SnCl_2$ was investigated using a Phipps & Bird standard 6-gang jar test apparatus (Richmond, VA) with six paddles (1in x 3in) and six 2.5 L B-KER acrylic square jars. 1 L of 50 µg/L Cr(VI)-spiked buffered water was filled into each jar after adjusting to desired pH. $SnCl_2$ dosages were prepared corresponding to the molar ratios of 0.5x, 1x, 1.5x, 3.5x, 5x, and 10x (x = Sn(II)/Cr(VI) stoichiometric ratio = 3/2 based upon EQN 2.3).

Half-reactions: $3Sn^{2+} \Rightarrow 3Sn^{4+} + 6e$ $E^0 = -462$ mV   (EQN 2.1)

$Cr_2O_7^{2-} + 14H^+ + 6e^- \Rightarrow 2Cr^{3+} + 7H_2O$ $E^0 = 1380$ mV   (EQN 2.2)

Overall equation: $3Sn^{2+} + Cr_2O_7^{2-} + 14H^+ \Rightarrow 3Sn^{4+} + 2Cr^{3+} + 7H_2O$ $E^0 = 918$ mV (EQN 2.3)
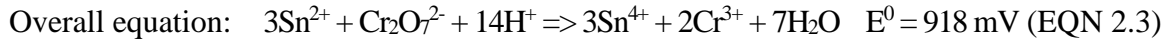
Cr(VI)-spiked waters and $SnCl_2$ were simultaneously added into six jars and stirred 10 minutes at 200 rpm for rapid mix. Two 30 mL solution aliquots were collected at 10 cm depth at different time intervals from 0 to 600 sec. pH, dissolved oxygen, and temperature are recorded right after 10-minute reaction. The experiments were conducted in triplicate and an experimental matrix had baseline conditions of pH=8.50$\pm$0.05, initial Cr(VI) concentration = 50 μg/L, DO level = 5.00$\pm$0.30 mg/L with buffered water source and $SnCl_2$ reagent grade.

Afterwards, Cr(VI) reduction by $SnCl_2$ was tested with different pH (7.50$\pm$0.05 and 9.50$\pm$0.05), Cr(VI) initial concentrations (25 and 100 μg/L), native Arizona groundwater, and $SnCl_2$ from Guard Product. Deoxygenated Cr(VI)-containing water and $SnCl_2$ solution were prepared for anaerobic experiment by covering the jar with parafilm and purging the solutions with high-purity N_2 gas for 30 minutes before the reduction experiment. One of the aliquots was kept non-filtered and another portion was filtered with 0.45 μm nylon membrane (GVS, Clifton, NJ).

1.3. Analytical Methods

The samples were acidified with ultrapure 2% HNO_3 (Sigma-Aldrich (ACS), 70%) and dissolved Cr(T) was measured along with other oxyanions (As(T) and W(T)) by Thermo-

Fisher Scientific X-Series 2 quadrapole ICP-MS equipped with Cetac ASX-520 auto-sampler.

Cr(VI) concentration was analyzed by the modified US EPA 7194A. 10 mL of effluent samples was mixed well with one 1,5-diphenylcarbazide HACH powder pillow (Loveland, CO) in a sample cell. This mixture was slowly swirled for 5 minutes to ensure the completion of bright purple Cr(VI)-DPC complex and 542 nm absorbance was immediately measured. Cr(VI) calibration curves for two water matrices were plotted using the absorbance of 2,5, 10, 25, 50, 100 μg/L Cr(VI) standards (Figure S1). Detection limits for this colorimetric method were determined as 4 ug/L for both buffered and challenge water. Trivalent chromium (Cr(III)) concentration was determined as the difference in the concentration of Cr(T) and Cr(VI).

pH and temperature were measured by a Beckman-Coulter pH probe (Brea, CA) which was calibrated with standard pH buffers of 4.0, 7.0, and 10.0. Electrical conductivity was determined using a VWR conductivity meter (Radnor, PA) and DO level was measured by an YSI optical DO meter (Yellow Springs, OH).

2.4. Thermodynamic and Kinetic Modeling

Equilibrium speciation of Cr and Sn species were calculated under different pH and redox conditions by Visual MINTEQ 3.1 (Gustafsson 2018). Input concentrations of all components were set equal to the experimental conditions: [Sn(II)] = 170 μg/L, [Cr(VI)] = 50 μg/L; [Na$^+$] = [HCO$_3^-$] = 5 mmol/L; [Cl$^-$] = 102 μg/L; [K$^+$] = 37.5 μg/L. Other parameters such as temperature and ionic strength were kept constant at 20°C and 0.025

M, respectively. Since $Cr(OH)_2^+$ and CrO_4^{2-} were considered as the major components of Cr(III) and Cr(VI) in Visual MINTEQ, all reactions contained Cr were defined by these species. Saturation indices for possible minerals formed during Cr(VI) reduction were estimated to elucidate which precipitations are over-saturated or under-saturated. Thermodynamic databases for Sn and Cr species were originally derived from MINTEQA2 (US EPA, VA) which revised using NIST version 6.0 and 7.0 databases.

Kinetics of Cr(VI) reduction was simulated based on an approach by Buerge and Hug, 1997 when they modeled Cr(VI) reduction by Fe(II). Assume that [Sn(II)]/[Cr(VI)] remains unchanged at constant c during the reaction. The redox reaction between $Cr_2O_7^{2-}$ and Sn^{2+} can be expressed as:

$$3Sn^{2+} + Cr_2O_7^{2-} + 14H^+ => 3Sn^{4+} + 2Cr^{3+} + 7H_2O$$
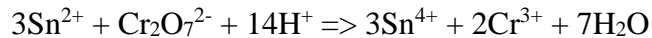
Generally, the rate expression can be written down as:

$$- d[Cr_2O_7^{2-}]/dt = k[H^+]^x[Sn^{2+}]^y[Cr_2O_7^{2-}]^z \qquad \text{(EQN S1.1)}$$

with x,y,z = the reaction orders with respect to $[H^+]$, $[Sn^{2+}]$, $[Cr_2O_7^{2-}]$

At pH of 7.5, 8.5, and 9.5, pH decreased slightly after $SnCl_2$ addition, therefore, $[H^+]$ can be assumed as a constant during the reaction. $[Sn^{2+}]_0/[Cr_2O_7^{2-}]_0$ is 10.5, 15, 30 thereby $[Sn^{2+}]$ is considered excessive to $[Cr_2O_7^{2-}]$ and remains unchanged during the reaction. Define the observed rate constant as $k_{obs} = k[H^+]^x[Sn^{2+}]^y$, the rate law is dependent only on $[Cr_2O_7^{2-}]$:

$$- d[Cr_2O_7^{2-}]/dt = k_{obs}[Cr_2O_7^{2-}]^z \qquad \text{(EQN S1.2)}$$

A linear equation can be derived by taking logarithm of both sides:

For constant [Sn^{2+}]: $\log k_{obs} = \log k' - x\, pH$ where $k' = k[Sn^{2+}]^y$ (EQN S1.3)

For constant pH: $\log k_{obs} = \log k'' + x\, \log[Sn^{2+}]$ where $k'' = k[H^+]^x$ (EQN S1.4)

Plotting $\log k_{obs}$ against $\log[Sn^{2+}]$ and pH, we can determine the reaction orders with respect to [Sn^{2+}] and [H^+]. Overall rate constant k can be calculated from the interceptions of these graphs.

CHAPTER 3. RESULTS AND DISCUSSION

3.1. Four Operational Models for SnCl₂ Treatment System

Four treatment scenarios involving Cr(VI) reduction were considered and represented in Figure 3.1. Scenario I illustrates the complete reducing conversion of Cr(VI) to Cr(III) by excessive Sn(II). Scenario II involves partial transformation of Cr(VI) to Cr(III) because ambient dissolved oxygen or other constituents exert a redox demand from Sn(II). Scenario III incorporates disinfection step after reduction/rapid mixing as the final step of the treatment train. Common disinfectants including free chlorine (OCl^-) or chloramine (NH_2Cl) are capable of re-oxidizing benign Cr(III) back into hazardous Cr(VI) (McNeill et al. 2012):

$$2Cr^{3+} + 3HOCl + 5H_2O => 2CrO_4^{2-} + 3Cl^- + 13H^+ \qquad E^0 = 4155 \text{ mV} \quad \text{(EQN 3.1)}$$

$$2Cr^{3+} + 3NH_2Cl + 8H_2O => 2CrO_4^{2-} + 3\,NH_3 + 3Cl^- + 13H^+ \qquad E^0 = 4062 \text{ mV} \quad \text{(EQN 3.2)}$$
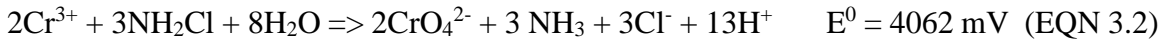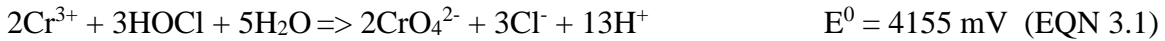
Scenario IV is quite similar to Scenario III, however, comprises a filtration system (cartridge filter/ceramic filter/dual-media filter)　　in order to remove particulate Cr(III) prior to disinfection tank. Filtration does prevent re-oxidation of Cr(III) to Cr(VI) by the disinfectants. Cr(III) is fairly insoluble under drinking water pH conditions:

$$Cr^{3+} + 3OH^- <=> Cr(OH)_3 \qquad K_{sp} = [Cr^{3+}][OH^-]^3 = 6.7 \times 10^{-31}$$

Salt River Project identified Scenario I and II as their preferred options because they represent operational responsibilities of water deliveries and are technically feasible to inject directly Sn(II) at the well-heads from the feed to the canals. Therefore, Scenario I and II are the focus of the chapter. In limited sets of experiments, we also investigated the

influence of filtration in Scenario IV, however did not disinfect the water because we only

wanted to confirm the presence and ability to lower down Cr(T) concentration by filtration.
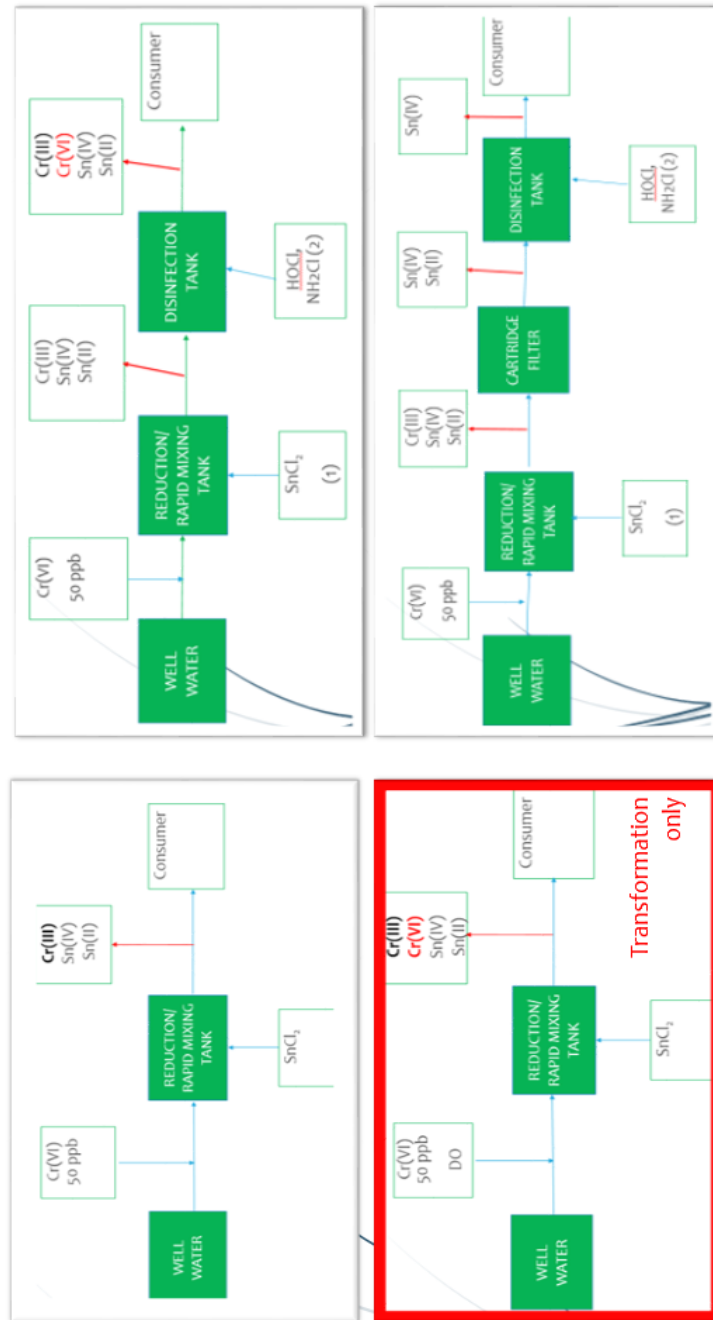
Figure 1. Redox Transformation of Cr(VI) to Cr(III) by SnCl₂ via

Four Treatment Scenarios

3.2. Scenario II: Model Buffered Ultrapure Water

The treatment goal for these reduction experiments was to achieve an effluent Cr(VI) concentration <10 µg/L. Figure 1a shows kinetics of Cr(VI) reduction by $SnCl_2$ dosing at 0.5x, 1x, 1.5x, 3.5x, 5x, and 10x. After adjusting pH to 8.5, the control experiments were performed with the absence of $SnCl_2$. Remaining Cr(VI) level fluctuates around the initial concentration (50-60 µg/L) and did not change over the course of the reaction. This implies Cr(VI) reduction to Cr(III) did not occur and Cr(VI) removal efficiency was essentially zero without $SnCl_2$ injection.

Testing at or above $SnCl_2$ stoichiometric dose, there was no significant effect on Cr(VI) residual level after 600 sec. All five experiments show excellent Cr(VI) removal of 90% and Cr(VI) concentration reached equilibrium at 5.25±0.96 µg/L after 600 sec. Dosing $SnCl_2$ at half stoichiometric ratio, only 50% Cr(VI) removal was observed and this dose could not reach the treatment target. The differences in Cr(VI) level were clearly observed during the first 60 sec and the kinetics of Cr(VI) reduction by $SnCl_2$ is extremely fast. Higher $SnCl_2$ doses increased drastically Cr(VI) reduction rate and little decrease in Cr(VI) level occurred between 120 and 600 sec. Stoichiometric dose of $SnCl_2$ is sufficient to reduce Cr(VI) concentration from 50 to 10 µg/L after 60 seconds in buffered water matrix. pH did not change substantially during 10-minute reaction.

3.3. Scenario II: Arizona groundwater

Figure 1b shows the changes of Cr(VI) concentration over 10 minutes of reaction using different $SnCl_2$ dosages. Low removal of Cr(VI) (~40-60%) was observed at or below 1.5 times $SnCl_2$ stoichiometric dose. Cr(VI) residual concentration declined sharply to 9 µg/L

(80% removal) within only 60 sec and 6 µg/L (90% removal) after 600 sec when 3.5 times Sn(II) stoichiometric dosage was added. Cr(VI) concentrations also attained equilibrium between 120 and 600 sec, as similar as in buffered water. Cr(VI) reduction rate increases significantly when increasing $SnCl_2$ doses and dosing 3.5 times Sn(II) stoichiometric dose is recommended to lessen Cr(VI) back to <10 µg/L. Negligible changes in pH were observed over the course of the reaction.

The kinetics of Cr(VI) reduction in Arizona groundwater is significantly lower than in buffered water, given that the similar $SnCl_2$ dose was applied. This can be explained by the fact that complex constituents of groundwater pressed a huge demand for $SnCl_2$. $SnCl_2$ continued dropping Cr(VI) concentration in challenge water whereas no changes in the model water were found after 600 sec.
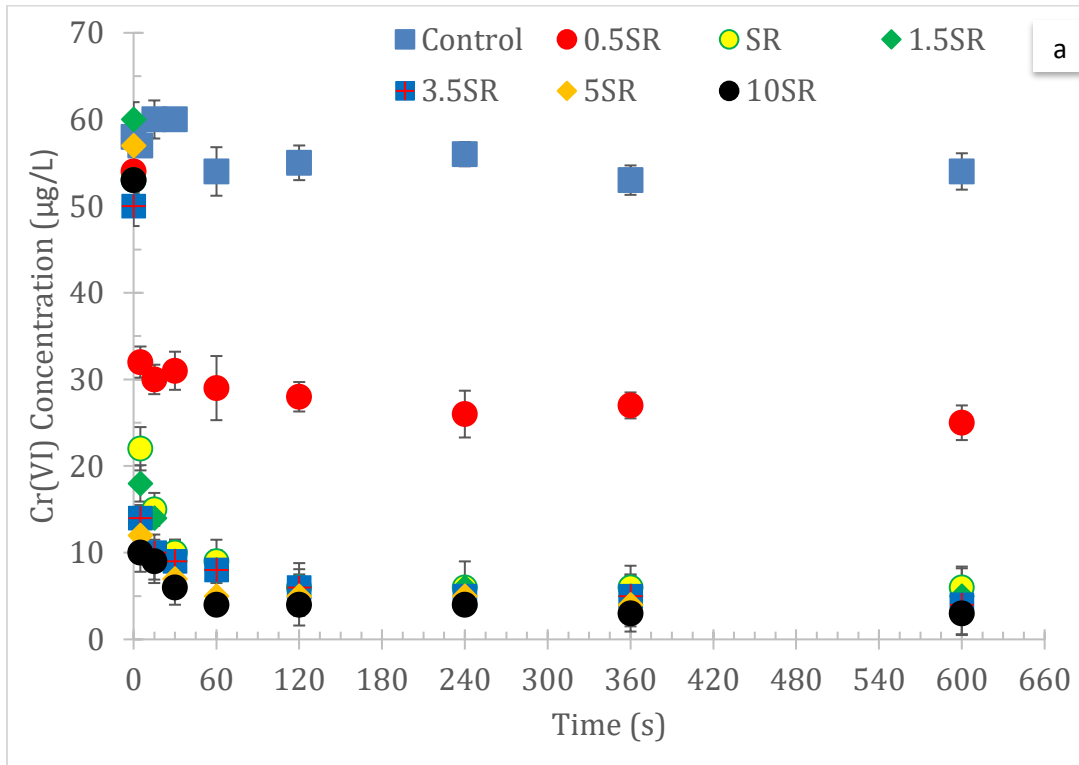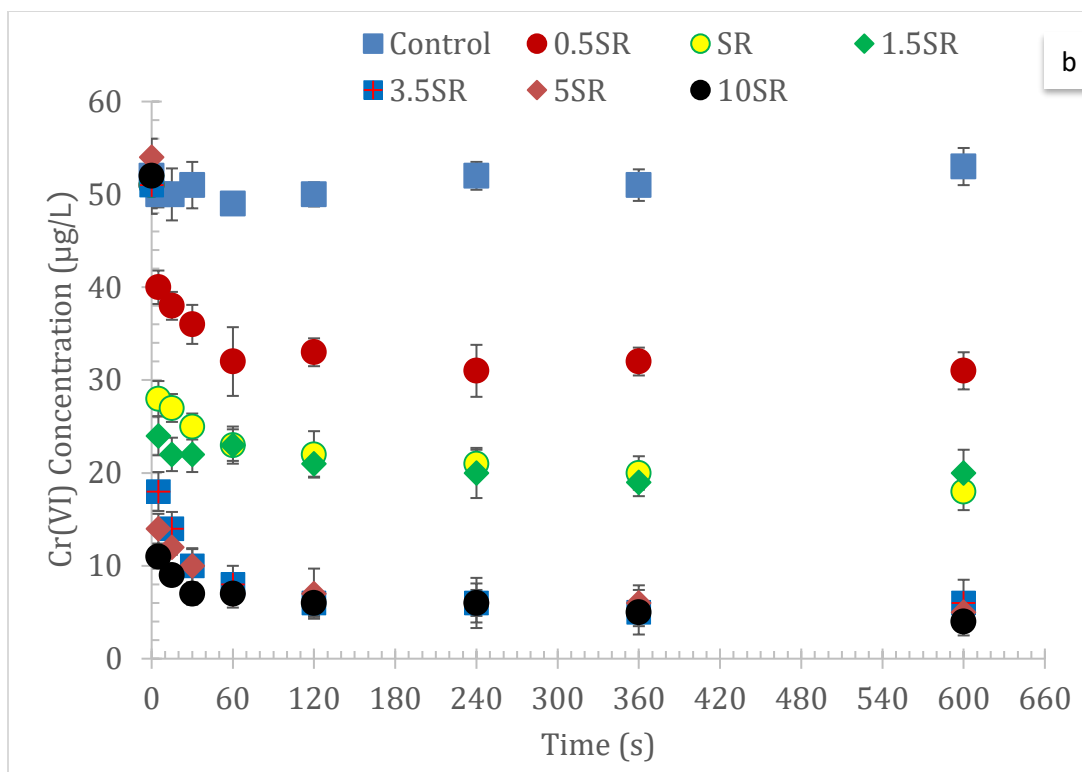
Figure 2. Kinetics of Cr(VI) Reduction by $SnCl_2$ ($[Cr(VI)]_0$ = 50-60 ppb) in a/5 mM

NaHCO$_3$ water and b/Arizona Groundwater

3.4. Effect of Water Chemistry on Cr(VI) Reduction Kinetics

Effect of pH

Figure 2a shows pH influence on Cr(VI) reduction kinetics by $SnCl_2$. Cr(VI) removal was found to be higher at pH = 9.5 than 8.5 and 7.5 at low Sn(II) doses. Using half-stoichiometric dose of $SnCl_2$, there were statistically significant differences between Cr(VI) residual levels (t = 120-600s) at pH = 9.5 (25.00 ± 0.58 µg/L), pH = 8.5 (19.50 ± 0.96 µg/L), and pH = 7.5 (17.5 ± 1.26 µg/L) (Figure S2b) ($p<0.05$). On the contrary, pH impacts slightly to Cr(VI) reduction when applying $SnCl_2$ dosages equal to or above stoichiometric ratio. Dosing $SnCl_2$ at stoichiometric ratio, there were statistical differences in the remaining Cr(VI) concentrations at pH=9.5 (6.50 ± 0.80 µg/L), pH =8.5 (7.50 ± 1.30 µg/L),

14

and pH=7.5 (8.25±1.50 µg/L) (Figure S2a) (p< 0.05). Cr(VI) treatment goal was reached within only 15 sec at pH = 9.5, while taking longer time of 60 sec at pH = 7.5. In summary, increasing pH improves Cr(VI) removal and dosing $SnCl_2$ at stoichiometric ratio achieves 10 µg/L final concentration. Faster reduction of Cr(VI) by $SnCl_2$ found at higher pH is comparable to the observations from previous studies on Cr(VI) reduction by Fe(II) (Sedlak and Chan 1998, Pettine et al. 1998, Schlauman and Han 2001).

Effect of Dissolved Oxygen

Figure 3b presents the effects of DO on Cr(VI) removal when dosing $SnCl_2$ from 0.5x to 10x. There was no statistical difference between Cr(VI) residual concentrations at equilibrium with DO=5.0 mg/L (22.25±2.96 µg/L) and DO=0.5 mg/L (18.50±2.58 µg/L)(p>0.05) (Figure S3b)**.** This indicates Cr(VI) removal extent is independent on DO level. Dosing $SnCl_2$ at or over stoichiometric ratio, Cr(VI) residual concentrations were found at 7.50±1.30 µg/L and 6.50±1.29 µg/L in oxygenated and deoxygenated conditions, respectively (Figure S3a). However, there were no significant differences in Cr(VI) concentration at t=120-600s (p>0.05). In brief, DO level does not affect Cr(VI) removal efficiency and dosing $SnCl_2$ at stoichiometric ratio is favorable to reduce Cr(VI) to less than 10 µg/L.

Effect of Initial Cr(VI) Concentration

Figure 2c shows Cr(VI) fractional removal was similar with varying Cr(VI) initial concentrations when the same $[Sn(II)]_0/[Cr(VI)]_0$ was applied. Sn(II)/Cr(VI) molar ratios correspond to 50% less or 200% higher in the testing with 25 and 100 ppb initial Cr(VI) jar tests, relative to the baseline 50 µg/L experiment. Consequently, this does require higher

SnCl$_2$ doses as Cr(VI) concentration increases. The arbitrary trend highlights that Cr(VI) removal is independent on its initial concentration. Adding SnCl$_2$ stoichiometric dosage, Cr(VI) concentration observed a substantial drop to 9.02±0.60 µg/L (80% reduction) after 60 sec, then reach the plateau at 7.50±1.29 µg/L (90% reduction) from 120 to 600 sec (Figure S4). This finding exemplifies the excellent removal of Cr(VI) by SnCl$_2$ since Cr(VI) concentration could plummet from 100 to below 10 µg/L after only 60 sec.

Effect of Water Matrix and Co-contaminant Oxyanions

Figure 2d compares Cr(VI) removal percentages by SnCl$_2$ in Arizona groundwater and buffered water. When dosing SnCl$_2$ at or less than stoichiometric ratio, Cr(VI) conversion to Cr(III) appeared to be kinetically slower and unable to achieve 10 µg/L treatment goal in groundwater. This result indicated background composition of Arizona groundwater does affect to the rate and extent of Cr(VI) reduction.

Co-occurring constituents in groundwater is possibly the dominant factor inhibited Cr(VI) reduction. Two common oxyanions - arsenic (As) and tungstate (W) were detected in the challenge water at 2-3 µg/L and 16-18 µg/L, respectively. Using SnCl$_2$ stoichiometric dosage, total concentrations of As and W decreased rapidly to 1 µg/L and 14 µg/L, respectively (Figure S5). This reveals 60% of W removal and 20% of As removal, thus promotes further investigations into W remediation by SnCl$_2$. Lower removal of Cr(VI) in Arizona groundwater can be explained by the competition of WO_2^{2-} and AsO_4^{3-} with $Cr_2O_7^{2-}$ for Sn^{2+} scavenging or the adsorption into the formed precipitates: $Cr(OH)_3$, Cr_2O_3, $Sn(OH)_4$, SnO_2, $Sn(OH)_2$, and their associated co-precipitations. Slight decrease in As and

W concentrations after adding $SnCl_2$ propounds the primary mechanism for removing these oxyanions is adsorption process.

3.5. Comparison of Filtered and Non-filtered Samples

Figure 2e compares Cr(VI) residual concentration in filtered and non-filtered samples after reacting with different $SnCl_2$ doses. In buffered water, filtration did not enhance Cr(VI) removal when dosing $SnCl_2$ at or over stoichiometric ratio. The difference in Cr(VI) removal was most obvious at half-stoichiometric dose of $SnCl_2$ with 61% and 72% for non-filtered and filtered samples, respectively. Figure S6 describes Cr(VI) reduction kinetics in filtered and non-filtered samples using $SnCl_2$ stoichiometric dosage. Between 120s and 600s, Cr(VI) concentrations reached equilibrium at 7.5±1.3 µg/L and 7.25±1.0 µg/L in filtered and non-filtered samples, respectively and p>0.05 proves there was no statistical difference between them. This can be explained by the fact that 0.45 µm membrane filter is not effective to discard all formed metal oxides/hydroxides whose particle sizes were possibly <0.45 µm. In short, 0.45 µm membrane filtration is not necessary enhance Cr(VI) removal, however, this practice is still suggested with smaller pore size to prevent the re-oxidation of Cr(III) to Cr(VI).

c

d
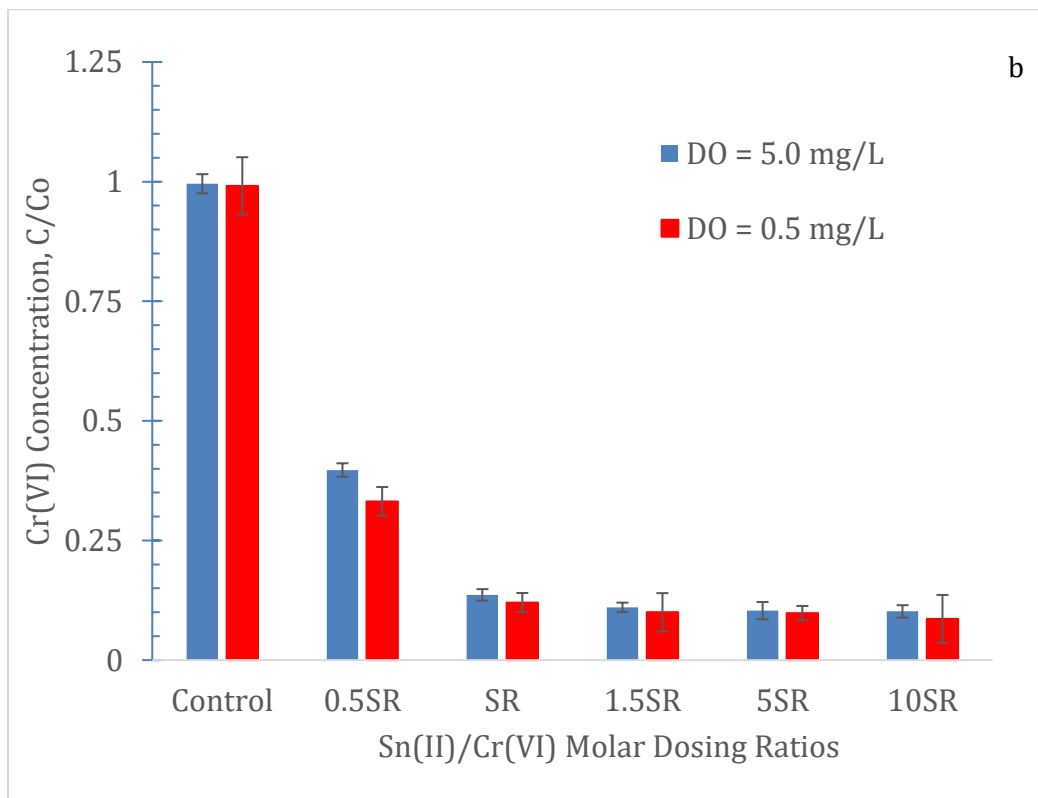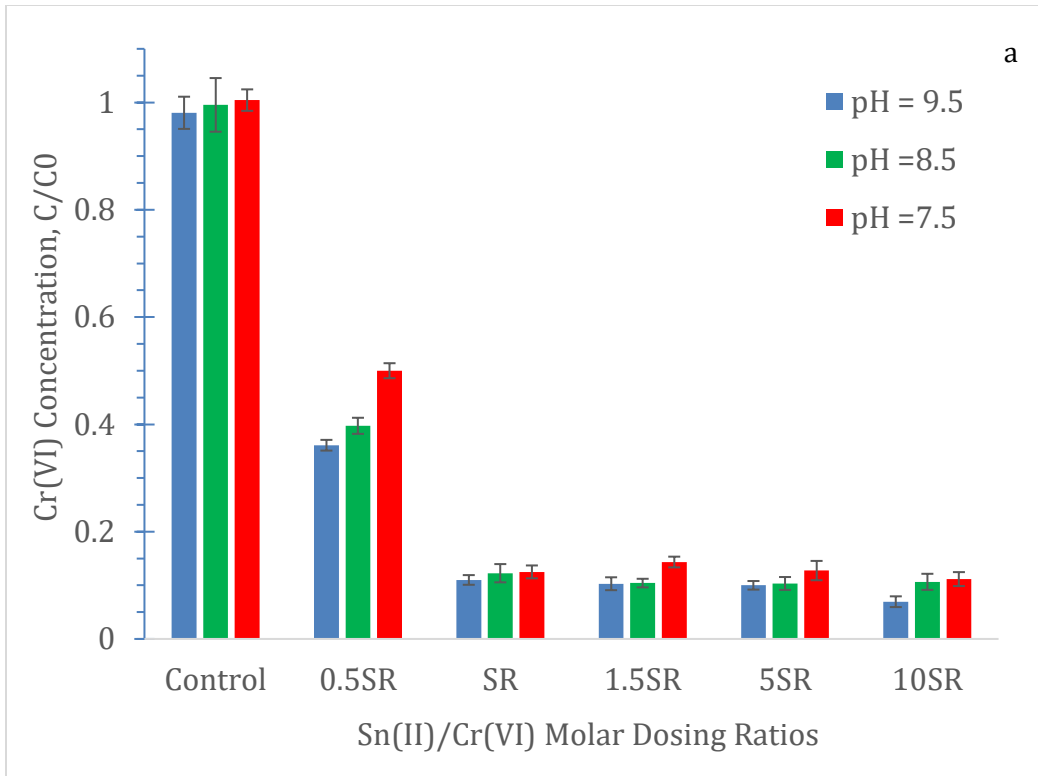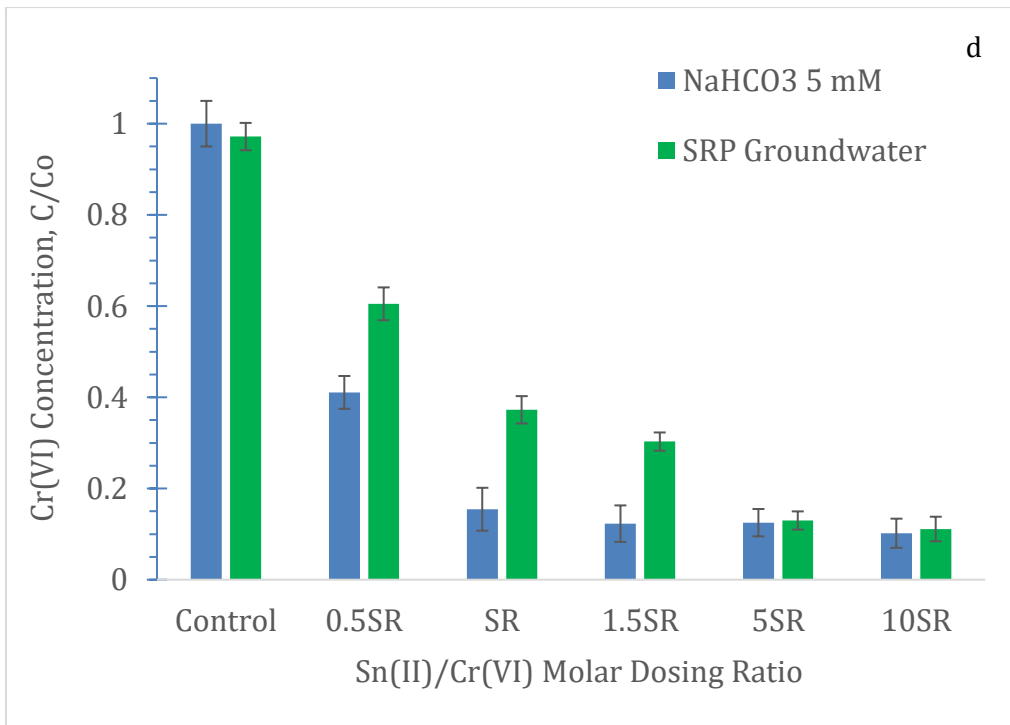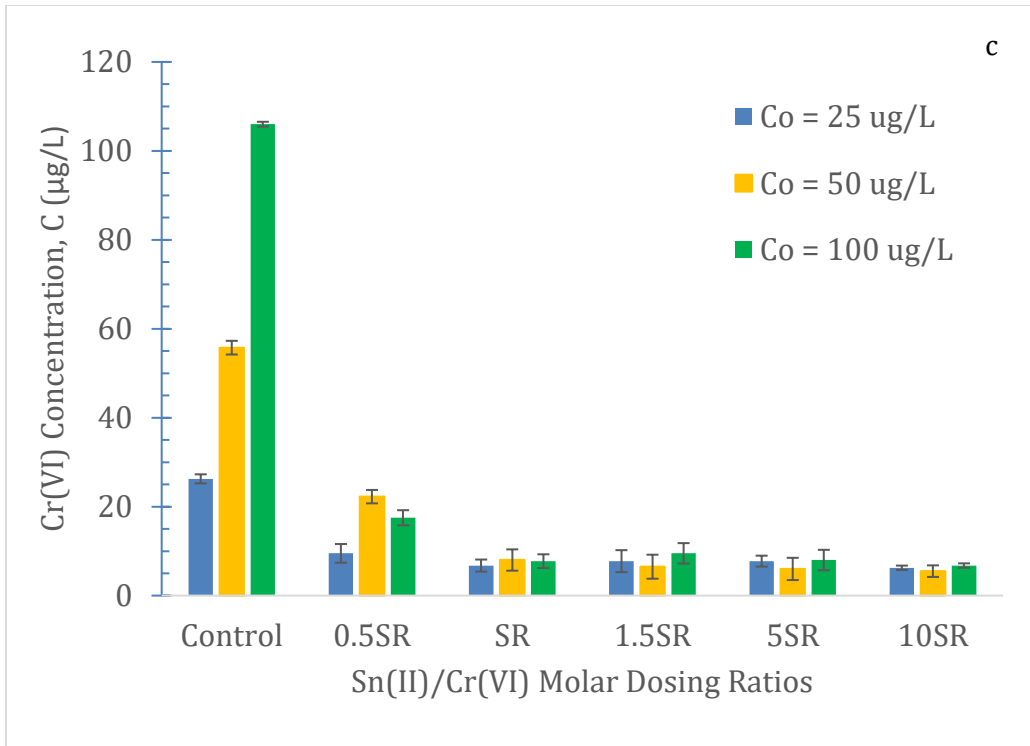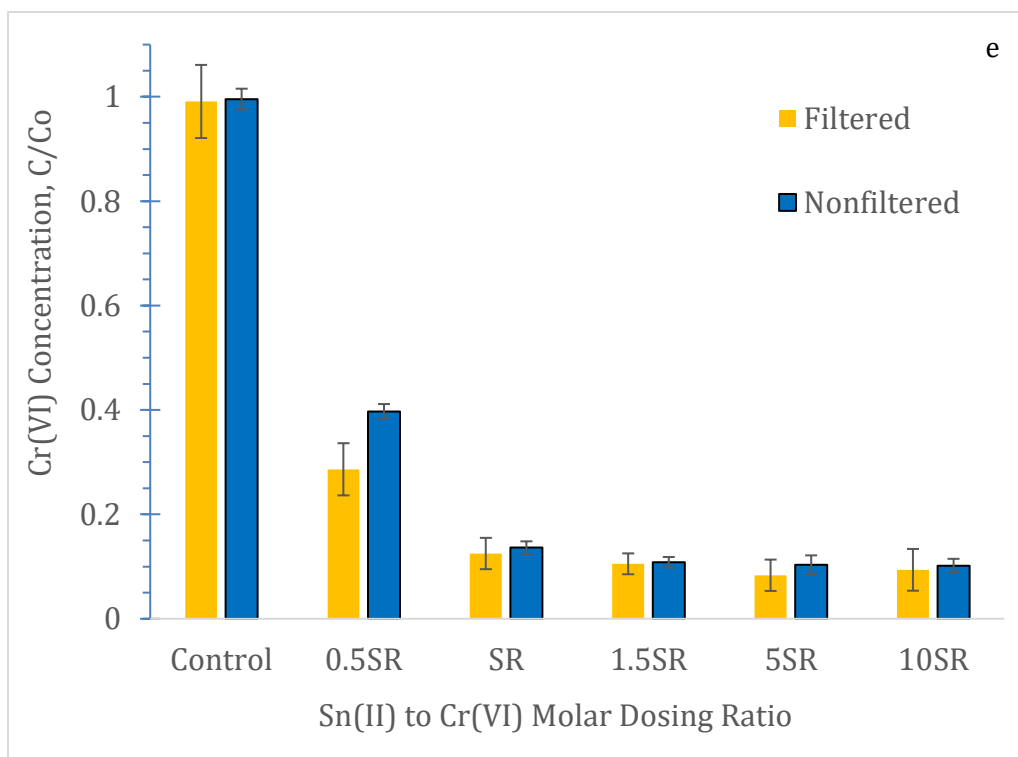
Figure 3. Effect of a/pH, b/DO Level, c/Initial Cr(VI) Concentration, d/Water Matrix,

e/Filtration Practice on Cr(VI) Removal Efficiency (t = 120-600 sec)

3.6. Comparison of SnCl₂ Reagent Grade and SnCl₂ Guard Product

SnCl$_2$ Guard Product expressed different potential for Cr(VI) reduction in buffered water

over time (Figure 3). Initially, both reagent and commercial SnCl$_2$ showed excellent Cr(VI)

removal within the first week after opening the bottle. Applying SnCl$_2$ stoichiometric

dosage resulted in around 90% and 40% removal in Experiment 1+2 (from 7/15/2018 to

7/22/2018) and Experiment 3+4 (from 7/23/2018 to 7/30/2018), respectively (Figure S7).

Reduction experiments with SnCl$_2$ commercial grade was tended to replicate 3 times,

however, an additional attempt was performed to validate the discrepancy between

Experiment 1+2 and Experiment 3. Dosing SnCl$_2$ over stoichiometric ratio followed the

same tendency except Cr(VI) removal increased notably to 70% in Experiment 3+4. This phenomenon can be due to the exposure of commercial $SnCl_2$ to the air decreased its reducing properties while $SnCl_2$ reagent grade was daily prepared. Accordingly, $SnCl_2$ Guard Product should be used during the first week after exposing to the atmosphere to obtain most effective Cr(VI) removal.
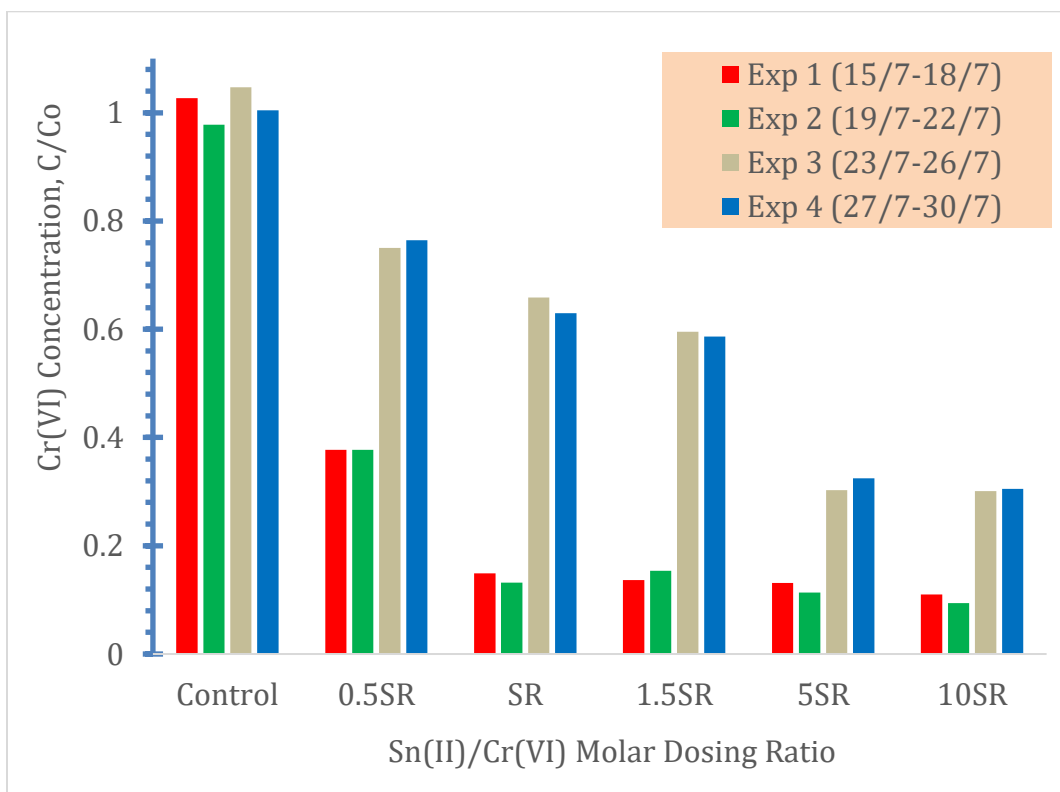
Figure 4. Four Consecutive Reduction Experiments Evaluating the Effectiveness of $SnCl_2$ Guard Product for Cr(VI) Removal in Buffered Water

3.7. Thermodynamic and Kinetic Modeling

Thermodynamic model

Equilibrium modeling of 272 µg/L dissolved $SnCl_2$ reacting with 50 µg/L Cr(VI) in 5 mM $NaHCO_3$ water at fixed pH = 8.5, ionic strength = 0.025 M, temperature = 20°C was

performed. In an open-to-atmosphere system, the solution has an equilibrium p_e of 6.29 (or a redox potential (E_h) of 365 mV). Thermodynamics predicted that Cr(VI) existed predominantly as CrO_4^{2-} (98.04%) whereas Cr(III) presented mainly as $Cr(OH)_3$ (aq) (99.04%). Sn(IV) distributed in the form of $H_2Sn(OH)_6$ (99.39%) whereas excessive Sn(II) formed $Sn(OH)_2$ (89.47%) and $Sn(OH)_3^-$ (10.52%).

Figure 4 represents Cr speciation versus E_h ranging from -1000 mV to 1000 mV. The concentrations of Cr(III) species reached their peaks while the concentrations of Cr(VI) species tended to drop when E_h decreased from 350 mV to -1000 mV. In addition, Cr(VI) removal is ineffective at highly oxidizing condition (E_h = 350-1000 mV). Dosing $SnCl_2$ at stoichiometric dose (E_h = 365 mV), Cr(VI) level decreased to close or below the treatment target of 1.92×10^{-7} M (10 µg/L).

Modeled [Total residual Cr(VI)] = 2.26×10^{-7} M can be calculated from individual species as the sum of $2[Cr_2O_7^{2-}]$, $[CrO_4^{2-}]$, $[CrO_3Cl^-]$, $[NaCrO_4^-]$, $[KCrO_4^-]$, $[KCr_2O_7^-]$, $[HCrO_4^-]$, and $[H_2CrO_4]$. The model also shows an effective Cr(VI) reduction (~80%) and agrees well with Cr(VI) remaining concentration of 1.44×10^{-7} M from the experiment. Modeled [Total formed Cr(III)] = 7.36×10^{-7} M was calculated from the sum of $[Cr(OH)_{3(aq)}]$, $[Cr(OH)_4^-]$, $[Cr^{3+}]$, $[Cr_2(OH)_2^{4+}]$, $[Cr_3(OH)_4^{5+}]$, $[Cr(OH)^{2+}]$, $[Cr(OH)_2^+]$ and $[CrCl^{2+}]$. This value is relatively close to Experimental [Total formed Cr(III)] (8.17×10^{-7} M), which confirms Cr(VI) reduction to Cr(III) is close to completion.

[Total residual Cr(VI)] decreases steadily and [Total formed Cr(III)] reaches maximum when pe declines to <6.90 (corresponding to E_h >= 400 mV). This result lined up with the experimental results since Sn(II) stoichiometric dose possesses pe = 6.30 < 6.90 reduces

dramatically Cr(VI) to 7 µg/L which is under the treatment goal. Table 1 provides pe ranges that result in different precipitates of Cr(III), Sn(II), and Sn(IV), and pe > 6.93 did not observe any solid forms of Cr(III). Thus dosing Sn(II) over stoichiometric ratio, which provides pe < 6.90, will lead to a greater capacity of Cr(VI) reduction to Cr(III).

Visual MINTEQ was also used to model the fate of As and W during Cr(VI) reduction by SnCl$_2$. A single solution condition was modeled with [As(V)] = 18 µg/L and [W(VI)] = 3 µg/L. These concentrations were selected because they approximates the typical conditions in Arizona groundwater. [Total residual Cr(VI)] was estimated to be 2.78 x 10^{-7} M in the simulated groundwater, which is moderately higher than 2.36 x 10^{-7} M in the buffered water. The addition of AsO$_4^{3-}$ and WO$_4^{2-}$ exerts an electron demand from Sn^{2+} and therefore decrease considerably the removal of Cr(VI). Therefore, thermodynamic model also concluded that lower Cr(VI) removal was observed in complex Arizona groundwater compared with buffered water, and As(V) and W(VI) competes with Cr(VI) for Sn(II) uptake.

Table 1. Predictions of Cr(III), Sn(II), Sn(IV) Mineral Phases with Respect to pe Value

pe value	Cr(III) precipitates	Sn(II) precipitates	Sn(IV) precipitates
-17.24 to -10.34	Cr(OH)$_3$, Cr$_2$O$_3$	Sn(OH)$_2$, SnO	No
-10.34 to -7.75	Cr(OH)$_3$, Cr$_2$O$_3$	No	H$_2$Sn(OH)$_6$
-7.75 to 6.93	Cr(OH)$_3$, Cr$_2$O$_3$	No	H$_2$Sn(OH)$_6$, SnO$_2$
6.93 to 17.34	No	No	H$_2$Sn(OH)$_6$, SnO$_2$
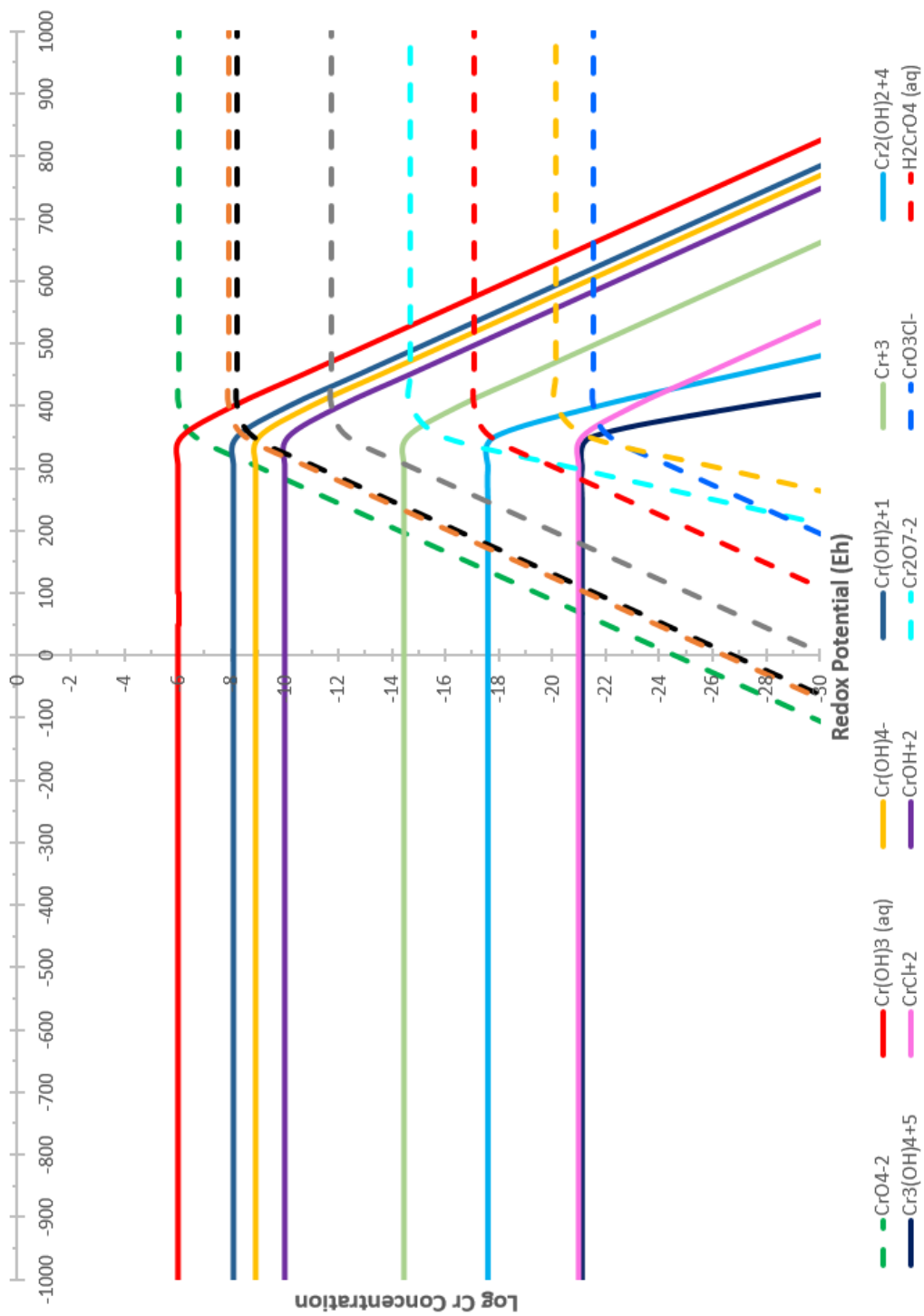
Figure 5. Equilibrium Modeling of Cr Speciation during SnCl$_2$ Treatment by

Visual MINTEQ

Kinetic model

Cr(VI) reduction data (from different [SnCl$_2$] and pH experiments) were collected to determine [Cr$_2$O$_7^{2-}$], [Sn^{2+}], and [H$^+$] reaction orders. Cr(VI) reduction kinetics occurred mainly in the first minute, so these data points used to fit corresponds to this time interval. Pseudo third-order kinetics, which has the root of $1/[Cr_2O_7^{2-}]^2 = 1/[Cr_2O_7^{2-}]_0^2 + 2k_{obs}t$, correlated consistently with our observed data. Under [Sn^{2+}]$_0$/[Cr$_2$O$_7^{2-}$]$_0$ = 10.5, 15, 30, plotting $1/[Cr_2O_7^{2-}]^2$ versus time yields good linear fits with experimental data ($R^2 = 0.92$-0.94) (Figure S9). This implies the reaction follows third order with respect to [Cr$_2$O$_7^{2-}$].

Table S2 shows the estimated k_{obs} corresponding to different [Sn^{2+}]$_0$. The observed rate constant declines from 2.339 to 1.656 and 1.340 $\mu M^{-2}.s^{-1}$ when [Sn^{2+}]$_0$ decreases from 10 to 5 and 3.5 times stoichiometric dose. This indicates that Cr(VI) reduction occurred more rapidly with higher Sn^{2+} dosage, which is consistent with the trend of experimental data.

The dependence of k_{obs} on initial Sn(II) concentration can be analyzed by plotting log k_{obs} against log [Sn^{2+}]. The regression line has $R^2 = 0.97$ depicts that the reaction order with respect to [Sn^{2+}] is approximately 0.5 (Figure 5a).

Using the data from [Sn^{2+}]$_0$/[Cr$_2$O$_7^{2-}$]$_0$ = 30 experiments, $1/[Cr_2O_7^{2-}]^2$ versus time graph was plotted under different pH values, and the regression lines show a linear relationship ($R^2 = 0.93 - 0.98$) (Figure S10). Observed rate constants corresponding to pH = 7.5, 8.5, and 9.5 were estimated from the regression line slopes in Table S3. It is evident that k_{obs} values were higher with increasing pH, which indicates Cr(VI) reduction happens significantly faster at high pH environment. Specifically, k_{obs} obtained at pH = 9.5 is about 3 times higher than at pH = 7.5.

Plotting log k_{obs} versus pH resulted in a straight line with $R^2 = 0.93$, and [H$^+$] reaction order can be achieved from the slope of the regression line (-0.25) (Figure 5b). Since [Sn^{2+}] was assumed to be constant during the whole reaction, and the overall rate constant can be calculated from the line interception: 0.146 $\mu M^{-2.25}s^{-1}$.
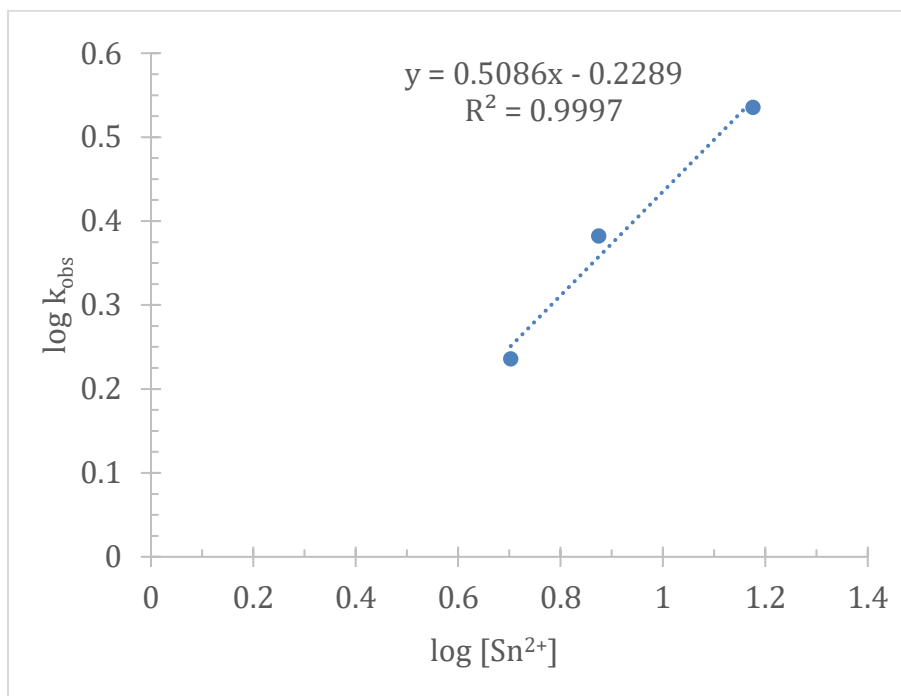
Figure 6a. Determination of [Sn^{2+}] Reaction Order for Cr(VI) Reduction by SnCl$_2$

at pH = 8.50±0.05
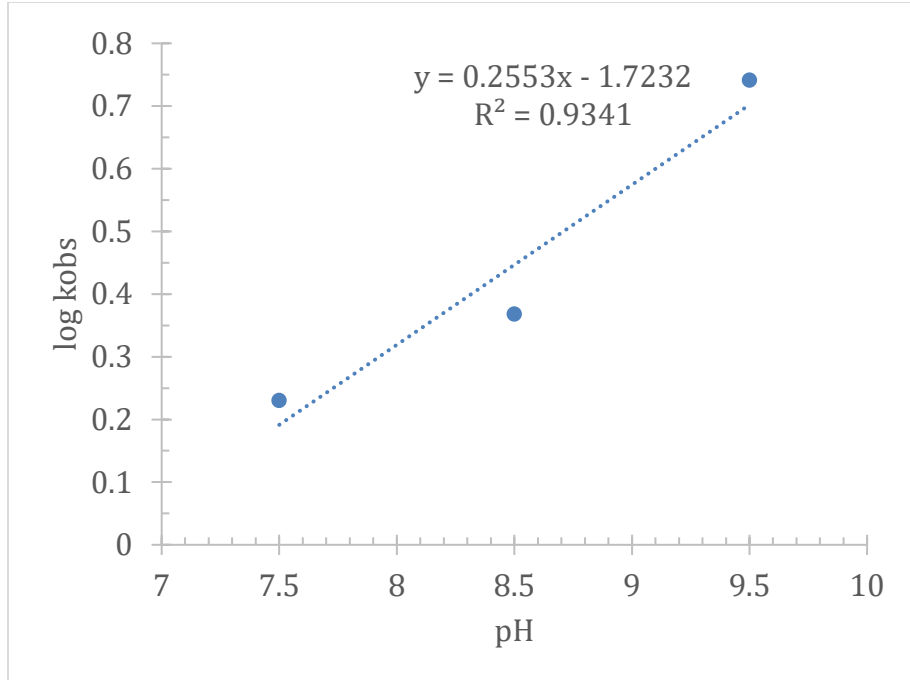
Figure 6b. Determination of $[H^+]$ Reaction Order for Cr(VI) Reduction by $SnCl_2$

$([Sn^{2+}]_0/[Cr_2O_7^{2-}]_0 = 30)$

Overall, the rate expression of Cr(VI) reduction by Sn(II) can be empirically determined

under experimental conditions as:

$-d[Cr_2O_7^{2-}]/dt = -d[Sn^{2+}]/3dt = k[H^+]^{-0.25}[Sn^{2+}]^{0.5}[Cr_2O_7^{2-}]^3$ with k = 0.146 $\mathbf{\mu M}^{-2.25}s^{-1}$

Assume $[Sn^{2+}]/[Cr_2O_7^{2-}]$ maintains at a constant ratio c during the reaction, the root can be

given by:

$1/[Cr_2O_7^{2-}]^{2.5} = 1/[Cr_2O_7^{2-}]_0^{2.5} + 2.5ck[H^+]^{-0.25}t$ (EQN 3.1)

or $[Cr_2O_7^{2-}] = [Sn^{2+}]/c = (1/(1/[Cr_2O_7^{2-}]_0^{2.5} + 2.5ck[H^+]^{-0.25}t))^{1/2.5}$ ($\mathbf{\mu M}$).   (EQN 3.2)

Stoichiometric model. Experimental data for Sn(II) stoichiometric dosage were used to fit

into the kinetic model and c = 3.6 showed an excellent fit with Cr(VI) reduction data.

Therefore, $Cr_2O_7^{2-}$ concentration can be calculated at a particular time in the stoichiometric experiment as follows:

$$[Cr_2O_7^{2-}] = [Sn^{2+}]/3.6 = (1/(1/[Cr_2O_7^{2-}]_0^{2.5} + 9k[H^+]^{-0.25}t))^{1/2.5} \text{ (μM)} \qquad \text{(EQN 3.3)}$$

Over-stoichiometric model. The fundamental idea to build over-stoichiometric model is based on the calibration of the constant c when $SnCl_2$ is not dosed at stoichiometric ratio $([Sn^{2+}]_0/[Cr_2O_7^{2-}]_0 \neq 3)$. From the experiment, Cr(VI) reduction occurred more rapidly with increasing $[Sn^{2+}]_0$, thus Sn(II) dosage is considered as a positively impacted parameter. The constant ratio c was then adjusted proportionally to Sn(II) dosages in Table 2.

Table 2. Kinetic Equations for Over-stoichiometric Sn(II) Dosages

Experiments	Adjusted c	Kinetic equations
$[Sn^{2+}]_0/[Cr_2O_7^{2-}]_0$ $= 4.5$	5.4	$[Cr_2O_7^{2-}] = [Sn^{2+}]/5.4$ $= (1/(1/[Cr_2O_7^{2-}]_0^3 + 13.5k[H^+]^{-0.35}t))^{1/3}$ (μM) **(EQN 3.4)**
$[Sn^{2+}]_0/[Cr_2O_7^{2-}]_0$ $= 10.5$	12.6	$[Cr_2O_7^{2-}] = [Sn^{2+}]/10.5$ $= (1/(1/[Cr_2O_7^{2-}]_0^3 + 31.5k[H^+]^{-0.35}t))^{1/3}$ (μM) **(EQN 3.5)**
$[Sn^{2+}]_0/[Cr_2O_7^{2-}]_0$ $= 15$	18	$[Cr_2O_7^{2-}] = [Sn^{2+}]/18$ $= (1/(1/[Cr_2O_7^{2-}]_0^3 + 45k[H^+]^{-0.35}t))^{1/3}$ (μM) **(EQN 3.6)**

$[Sn^{2+}]_0/[Cr_2O_7^{2-}]_0$	36	$[Cr_2O_7^{2-}] = [Sn^{2+}]/36$
$= 30$		$= (1/(1/[Cr_2O_7^{2-}]_0^3 + 90k[H^+]^{-0.35}t))^{1/3}$ **(µM)** **(EQN 3.7)**

Both stoichiometric and over-stoichiometric models correlate well to experimental Cr(VI) concentration, as illustrated in Figure 6. At high Sn(II) dosages ($[Sn^{2+}]_0/[Cr_2O_7^{2-}]_0 = 15$ and 30), the models underestimated Cr(VI) concentrations slightly, however, the difference between observed and predicted Cr(VI) concentration is only within 1 µg/L at all time intervals. Therefore, stoichiometric- and non-stoichiometric models are applicable to simulate Cr(VI) reduction by SnCl₂ under our experimental conditions.
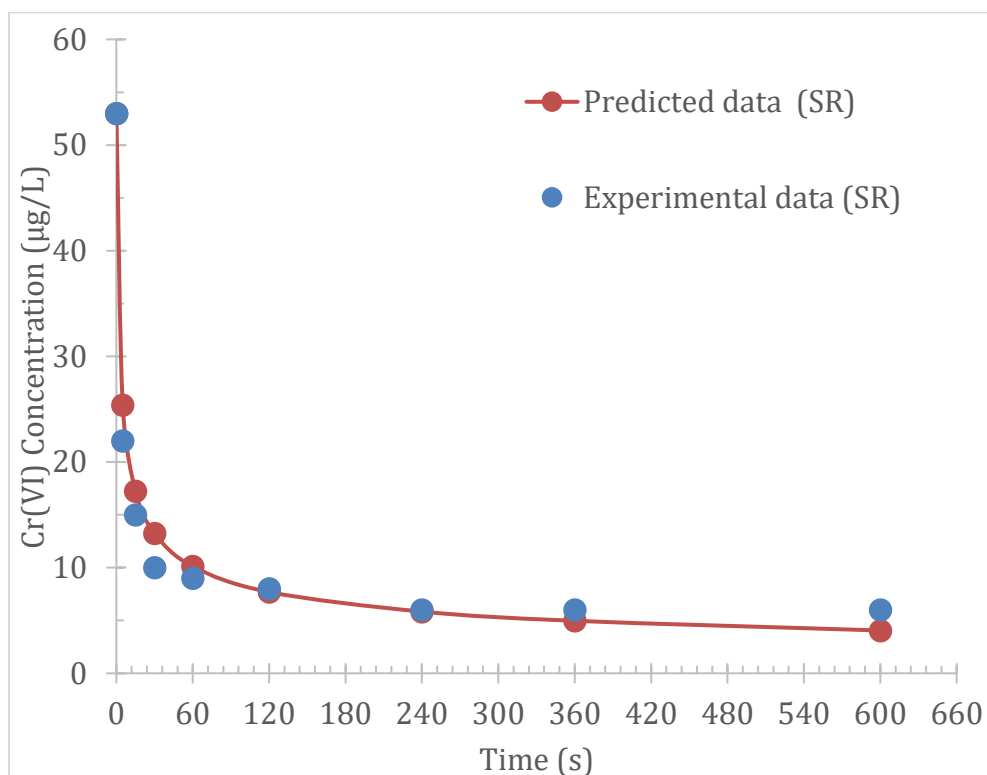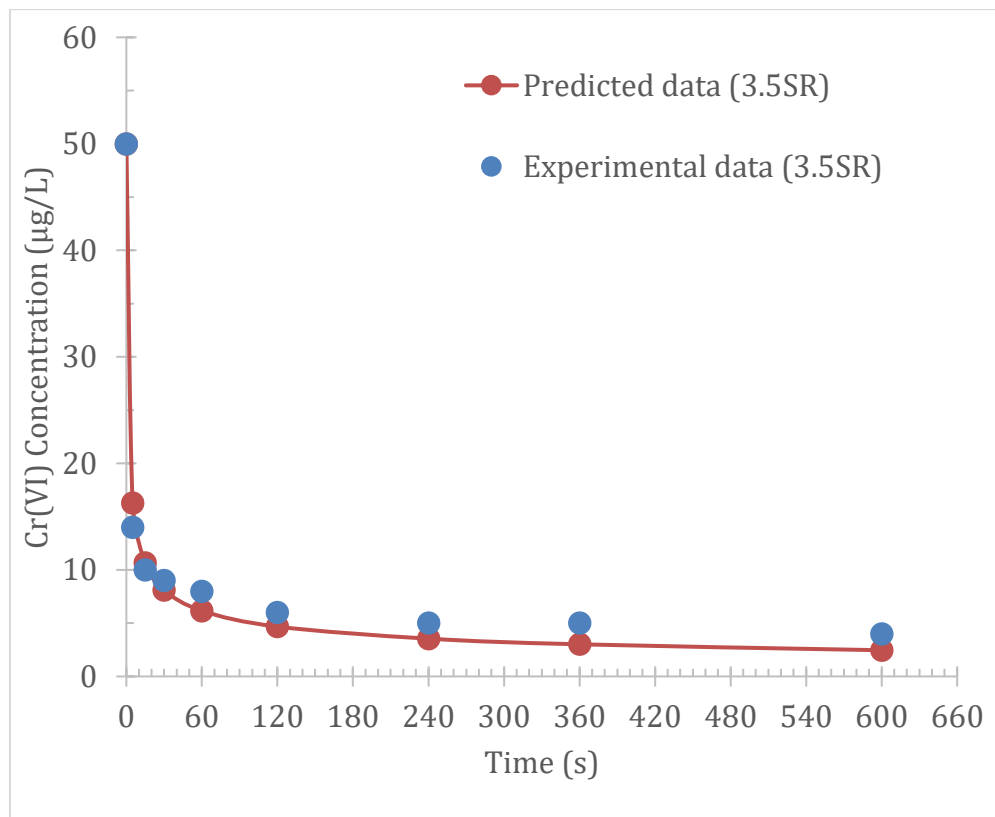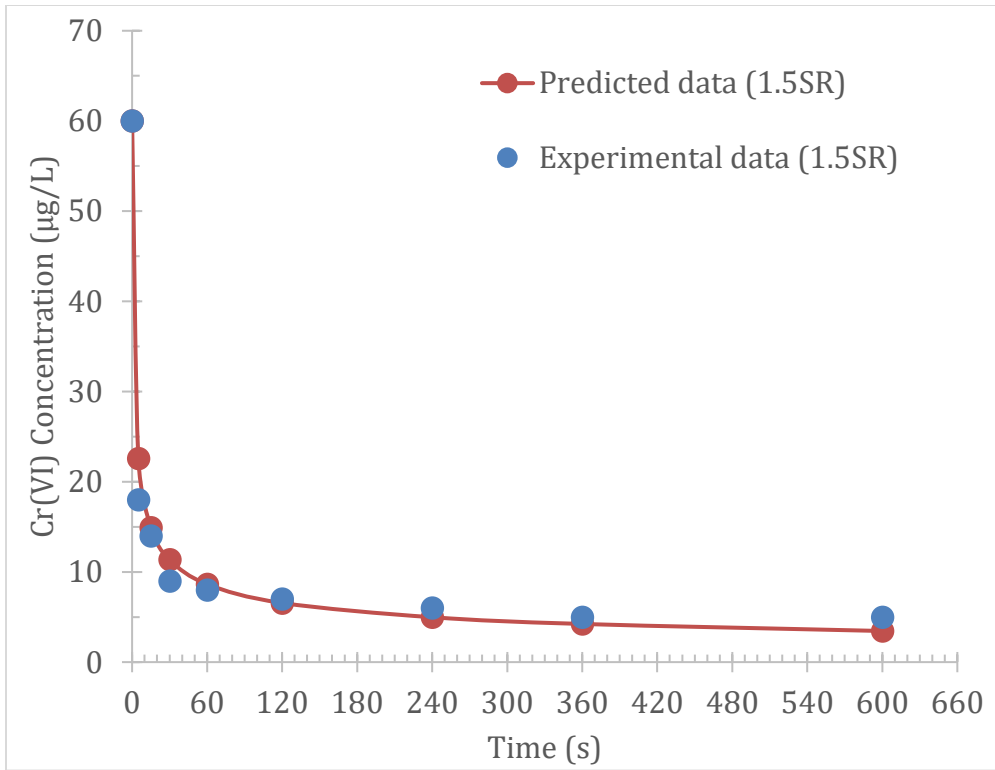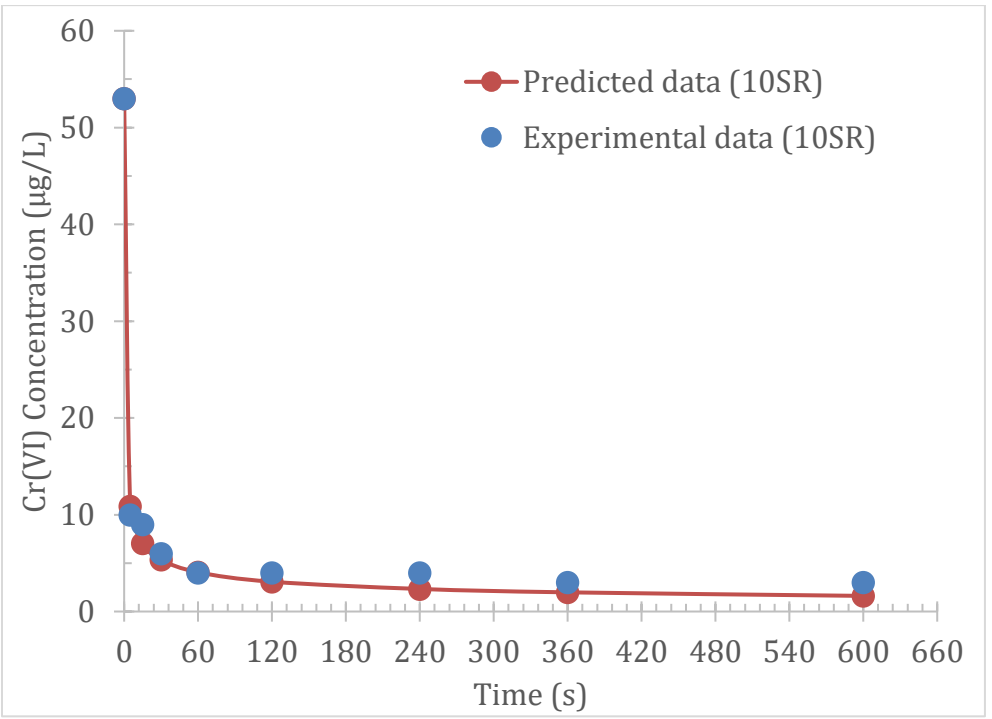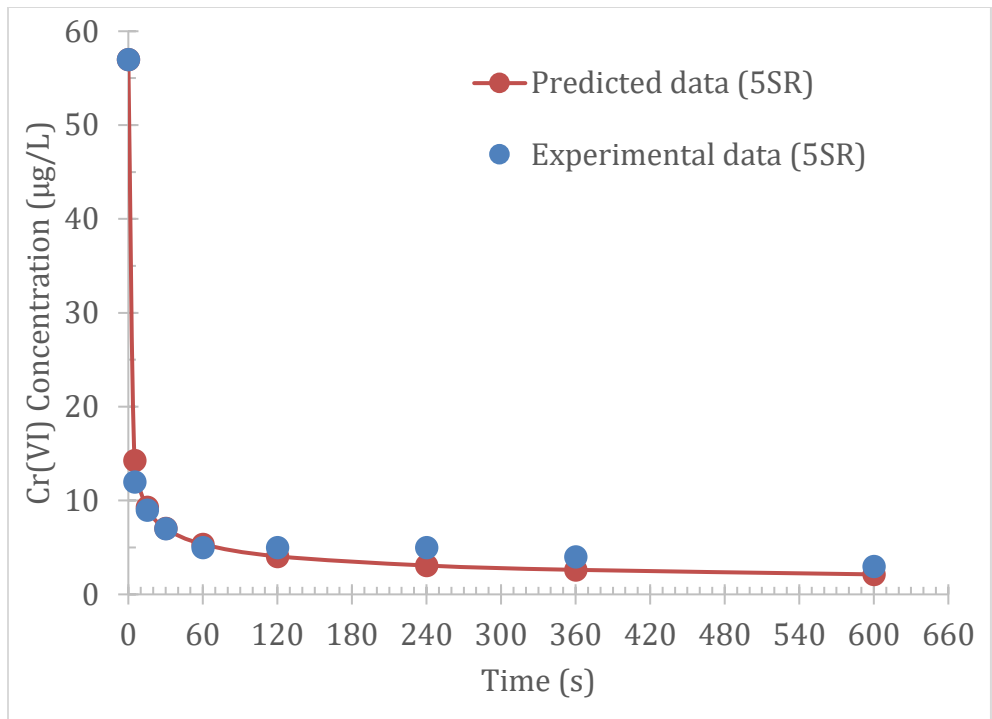
Figure 7. Comparison of Experimental and Modeled Cr(VI) Concentrations vs Time with

$[Cr(VI)]_0 = 50\ \mu g/L$ and pH $= 8.50\pm0.05$

31

These models are really useful to quantify the reaction time would require to reach a specific Cr(VI) concentration with different Sn(II) doses and pH. For instance, Santan Generating Station (Gilbert, AZ) that has the cooling towers blowdown water with 25 µg/L Cr(VI) can produce waste stream with the same level (Bowen 2014). If the plant applied $SnCl_2$ treatment with $[Sn^{2+}]_0/[Cr_2O_7^{2-}]_0$ = 3, 4.5, 15, and 30, it would take around 29.79s, 19.86s, 6.00s, and 3.00s to reach the treatment goal of 10 µg/L, respectively. They also can predict the contact time of 47.24s and 105.76s to lower Cr(VI) to 10 µg/L for other groundwater matrices that have pH of 8.0 and 7.0, respectively.

3D kinetic simulations of Cr(VI) reduction were performed in Figure 7 to determine whether Cr(VI) would be completely removed with five high Sn(II) dosages of 2655, 3540, 8850, 14160, 17700 µg/L (corresponds to 15, 20, 50, 80, and 100 times stoichiometric ratio). Blue and orange regions of the graph represents the acceptable Cr(VI) residual level < 10 µg/L. These high doses of Sn(II) reached Cr(VI) treatment target within 2.5 sec and 90% Cr(VI) reduction within 120 sec, which are very short contact times. The model predicts that Cr(VI) removal reached completion at 600s using 8850, 14160, 17700 µg/L Sn(II) dosages.
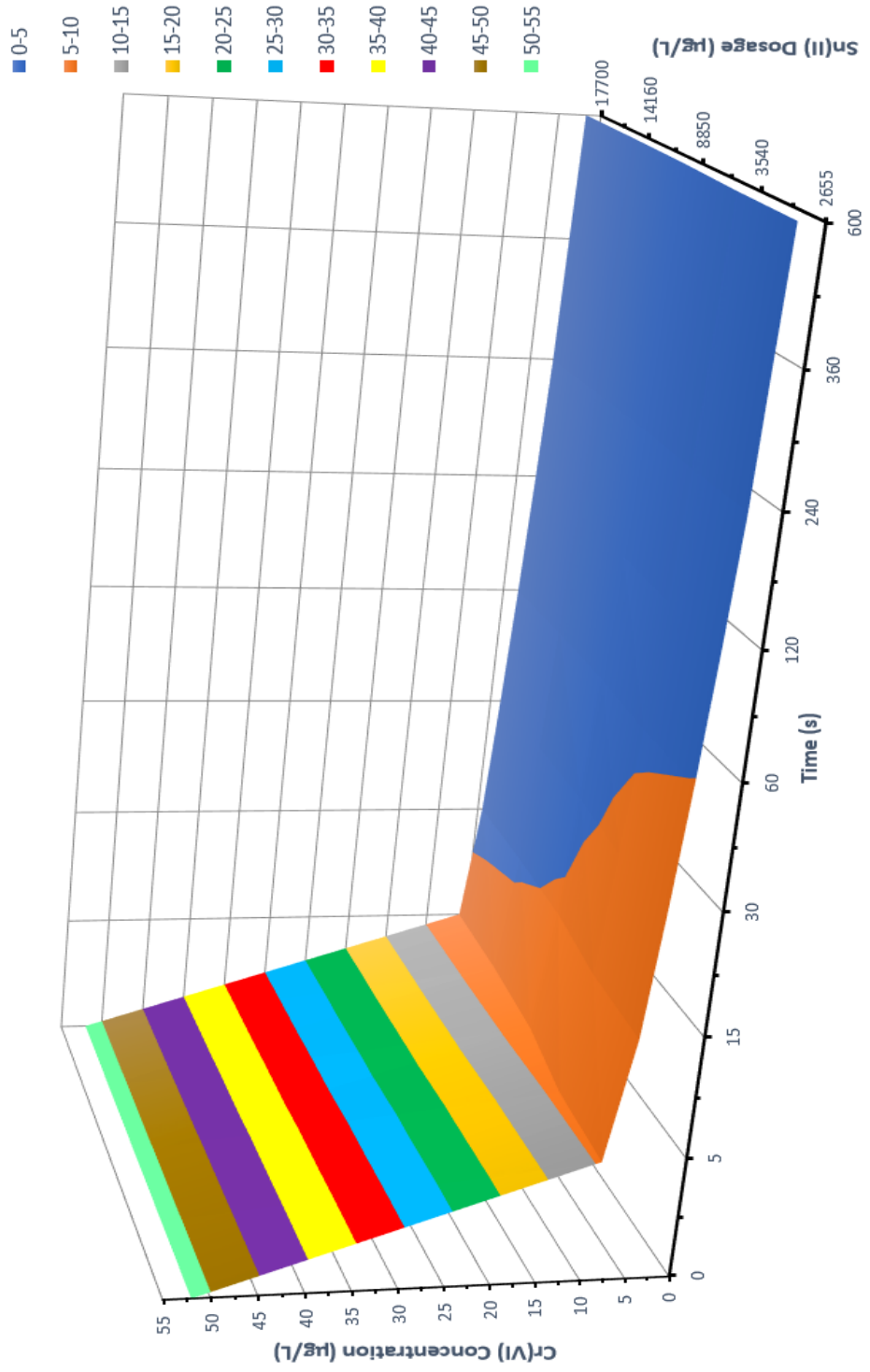
Figure 8. Kinetic Simulations of Cr(VI) Reduction by $SnCl_2$ During 10 Minutes of

Reaction ($SnCl_2$ dosages are corresponding to 15x, 20x, 50x. 80x, 100x)

33

CHAPTER 4. SUMMARY AND CONCLUSIONS

The major conclusions of this research include:

- ❖ SnCl$_2$ addition was demonstrated as a robust technology for Cr(VI) removal at SRP groundwater sites since applying 5 times stoichiometric dosage of Sn(II) is sufficient to reduce Cr(VI) to below 10 µg/L within only 15 seconds.

- ❖ Reduction kinetics of Cr(VI) increased slightly with high pH, whereas was essentially independent on initial Cr(VI) concentration and DO level. The existence of other oxyanions such as arsenic and tungstate resulted in a slower removal efficiency, and thereby background water composition does affect Cr(VI) reduction rate.

- ❖ SnCl$_2$ from Guard Product – a NSF certified vendor showed a decent removal of Cr(VI) within only one week after exposing to the atmosphere, and decreased its reduction capacity afterwards. No significant deviations between in residual Cr(VI) concentration between filtered and non-filtered samples were observed when dosing SnCl$_2$ higher than stoichiometric ratio, however, filtration practice is still suggested to eliminate the possibility that Cr(III) can re-oxidize to Cr(VI).

- ❖ Software simulation with Visual MINTEQ was performed to understand thermodynamic speciation of Cr and Sn and obtain the redox potential of <400 mV to reduce Cr(VI) effectively. At equilibrium, Cr(VI) existed primarily as CrO_4^{2} and Cr(III) presented mainly as Cr(OH)$_3$. Sn(IV) predominantly distributed in the form of Sn(OH)$_6^{2}$ and almost excessive Sn(II) formed Sn(OH)$_2$.

❖ Kinetic modeling determined empirically via the rate law: $r = -k[H^+]^{-0.25}[Sn^{2+}]^{0.5}[Cr_2O_7^{2-}]^3$ with overall rate constant: $k = 0.146\,\mu M^{-2.25}s^{-1}$. This rate expression is useful to predict the required contact time to achieve the treatment goal at a particular time and Sn(II) dosage. 3D graph simulates well Cr(VI) reduction by higher Sn(II) dosages and 50 times stoichiometric ratio were predicted to remove Cr(VI) completely after 10 minutes of reaction.

From these findings, in-situ chemical reduction by $SnCl_2$ proved applicable in SRP well-waters to achieve satisfactory Cr(VI) concentration. Further investigations should be conducted with two remaining operational models with the presence of disinfectants and cartridge filters and the re-oxidation process of Cr(III) to Cr(VI) to advanced $SnCl_2$ treatment system to pilot testing and full-scale implementation.

REFERENCES

1. Ball, J.W., Izbicki, J.A., 2004. Occurrence of hexavalent chromium in ground water in the western Mojave Desert, California. Appl. Geochem. 19, 1123–1135.

2. Blute, N.K. & Wu, Y., 2012. Chromium Research Effort by the City of Glendale California (Interim Report), Arcadis U.S. Inc., Los Angeles, California, US.

3. Bowen, A., 2014. Occurrence and Treatment of Hexavalent Chromium and Arsenic in Arizona Municipal and Industrial Waters, Master Thesis, Arizona State University.

4. Brandhuber, P., Frey M., McGuire M.J., Chao P., Seidel C., Amy G., Yoon J., Laurie McNeill, Banerjee K. Low-level hexavalent chromium treatment options: Bench-scale evaluation, AWWA Research Foundation, Denver.

5. Buerge, I. J.; Hug, S. J., 1997. Reduction of Chromium (VI) by Ferrous Iron, Environ. Sci. Technol., 31, 1426- 1432.

6. California Department of Public Health, 2016, Chromium-6 Drinking Water MCL, https://www.waterboards.ca.gov/drinking_water/certlic/drinkingwater/Chromium6.html (access 10/25/2018).

7. Chen, Z.F., Zhao, Y.S., Li, Q., 2015. Characteristics and kinetics of hexavalent chromium reduction by gallic acid in aqueous solutions. Water Sci. Technol. 71(11), 1694–1700.

8. Gustafsson J.P., 2006, Visual MINTEQ, KTH, Dept. Land and Water Resource Engineering, Stockholm.

9. Joe-Wong C., Brown Jr. G.E., Maher K. 2018. Kinetics and Products of Chromium(VI) Reduction by Iron(II-III)-Bearing Clay Minerals, Environ. Sci. Technol., 51:9817-9825.

10. Kaprara, E., Tziarou, N.,Kalaitzidou, K., Simeonidis, K., Balcells, L., Pannunzio, E.V., Zouboulis, A., Mitrakas, M., 2017. The use of Sn(II) Oxy-Hydroxides for Effective Removal of Cr(VI) from Water: Optimization of Synthesis Parameters, Sci. Total Environ., 605-606:190.

11. K. Wrobel, A.R.C. Escobosa, A.A.G. Ibarra, M.M. Garcia, E.Y. Barrientos, K. Wrobel, Mechanistic insight into chromium(VI) reduction by oxalic acid in the presence of manganese(II), J. Hazard. Mater. 300 (2015) 144–152.

12. Lai, H., McNeil, S., 2006. Chromium redox chemistry in drinking water systems. J. Environ. Eng., 132: 842–851.

13. Lai, K.C.K., Lo, I.M.C., 2008. Removal of chromium (VI) by acidwashed zero-valent iron under various groundwater geochemistry conditions. Environ. Sci. Technol. 42, 1238-1244.

14. Langlois, C.L., James, R.B., 2015. Chromium oxidation-reduction chemistry at horizon interfaces defined by iron and manganese oxides. Soil Sci. Soc. Am. J. 79, 1329-1339.

15. Lee, G. & Hering, J. G. 2003 Removal of chromium (VI) from drinking water by redox-assisted coagulation with iron (II). J. Water Supply Res. Tech. - AQUA 52(5), 319–332.

16. Li, X., Green, P.G., Seidel, C., Gorman, C., Darby, J.L., 2016. Meeting California s hexavalent chromium MCL of 10 ug/L using strong base anion exchange resin. J. Am. Water Work. Assoc. 108, 474-481.

17. Looney B.B., Denham M.E., Vangelas K.M., Bloom N.S., 2003. Removal of mercury from low-concentration aqueous streams using chemical reduction and air stripping, J. of Environ. Eng. 129 (9) 819–825.

18. Mathews, T.J.; Looney, B.B.; Bryan, A.L.; Smith, J.G.; Miller, C.L.; Southworth, G.R.; & Peterson, M.J., 2015. The Effects of a Stannous Chloride-Based Water Treatment System in a Mercury Contaminated Stream. Chemosphere, 138:190.

19. McGuire, M.J.; Blute, N.K.; Seidel, C.; Qin, G.; & Fong, L., 2006. Pilot-Scale Studies of Hexavalent Chromium Removal From Drinking Water. J. Am. Water Work. Assoc. 98:2:134.

20. Mullet, M., Boursiquot, S., & Ehrhardt, J.-J. (2004). Removal of hexavalent chromium from solutions by mackinawite, tetragonal FeS. Colloids and Surf. A, 244, 77–85.

21. Pettine, M., Dottone, L., Campanella, L., Millero, F.J., Passino, R., 1998. The reduction of chromium(VI) by iron(II) in aqueous solutions. Geochim. Cosmochim. Acta 62, 1509 -1519.

22. Pettine, M., Tonnina, D., & Millero, F. J. (2006). Chromium (VI) reduction by sulphur(IV) in aqueous solutions. Marine Chemistry 99, 31–41.

23. Pinakidou, F.; Kaprara, E.; Katsikini, M.; Paloura, E.C.; Simeonidis, K.; & Mitrakas, M., 2016. Sn(II) Oxy-Hydroxides as Potential Adsorbents for Cr(VI)-Uptake From Drinking Water: An X-Ray Absorption Study. Sci. Total Environ. 551–552:246.

24. Plummer S., Gorman C., Henrie T, Shimabuku K., Thompson R., Seidel. C., 2018 Optimization of strong-base anion exchange O&M. Water Res. 139, 420-433.

25. Qin, G., Mcguire, M.J., Blute, N.K., Seidel, C., Fong, L., 2005. Hexavalent chromium removal by reduction with ferrous sulfate, coagulation, and filtration: a pilot-scale study. Environ. Sci. Technol. 39, 6321–6327.

26. Rai, D., Sass, B.M., Moore, D.A., 1987. Chromium(III) hydrolysis constants and solubility of chromium hydroxide. Inorg. Chem. 26, 345-349.

27. Rivas, B.L., Aguirre, M. del C., 2010. Removal of As(III) and As(V) by tin(II) compounds. Water Res. 44, 5730–5739.

28. Schlautman, M.A., Han, I., 2001. Effects of pH and dissolved oxygen on the reduction of hexavalent chromium by dissolved ferrous iron in poorly buffered aqueous systems. Water Res. 35 (6), 1534–1546.

29. Sedlak, D.L., Chan, P.G., 1997. Reduction of hexavalent chromium by ferrous iron. Geochim. Cosmochim. Acta 61, 2185-2192.

30. Sedman, R.M., Beaumont, J., McDonald, T.A., Reynolds, S., Krowech, G., Howd, R., 2006. Review of the evidence regarding carcinogenicity of hexavalent chromium in drinking water. Environ. Sci. Health C 24 (1), 155-182.

31. U.S. Environmental Protection Agency, 2018. Definition and Procedure for the Determination of the Method Detection Limit, Revision 2, Washington DC.

32. Wazne, M., Jagupilla, S. C., Moon, D. H., Jagupilla, S. C., Christodoulatos, C., & Kim, M.G., 2007. Assessment of calcium polysulfide for the remediation of hexavalent chromium in chromite ore processing residue (COPR). J. Hazard. Mater. 143, 620–628.

33. Williams, A. G. B.; Scherer, M. M., 2001 Kinetics of Cr(VI) Reduction by Carbonate Green Rust. Environ. Sci. Technol. 35, 3488-3494.

34. Xu, X.R., Li, H.B., Gu, J.-D., 2004. Reduction of hexavalent chromium by ascorbic acid in aqueous solutions. Chemosphere 57, 609–613.

35. Yoon, J.; Amy, G.; Chung, J.; Sohn, J.; & Yoon, Y., 2009. Removal of Toxic Ions (Chromate, Arsenate, and Perchlorate) Using Reverse Osmosis, Nanofiltration, and Ultrafiltration Membranes. Chemosphere 77:2:228.

APPENDIX A

SUPPLEMENTAL CONTENTS

Determination of Method Detection Limit in Buffered Ultrapure Water and Arizona Groundwater

We determined MDL for both water sources (buffered water and challenge water) based on US EPA 821-R-16-006 method (US EPA, 2018). Firstly, the initial MDL was calculated by the standard deviation of the response and the slope of the calibration curve (Figure S1). Following that, we selected a Cr(VI) spiking level of 2-10 times the estimated MDL above at 10 µg/L (for both water matrices), and measured 15 spiked samples for Cr(VI) concentration. The samples used for MDL determination were prepared in different 7 days. The MDLs based on the spiked samples were calculated as below:

$$MDL_s = t_{(n-1, \, 1-\alpha = 0.99)} S_s$$

where: MDL_s = the method detection limit based on the spiked samples

$t_{(n-1, \, 1-\alpha = 0.99)}$ = Student's t-value appropriate for a single-tailed 99th percentile

S_s = sample standard deviation of the replicate spiked sample analyses

For Buffered Ultrapure Water

Sample #	C (ppb)	Abs
1	8.190	0.017
2	9.619	0.02
3	9.143	0.019
4	10.095	0.021
5	8.667	0.018
6	9.143	0.019
7	10.571	0.022
8	9.143	0.019
9	10.095	0.021
10	11.048	0.023
11	12.476	0.026
12	10.571	0.022
13	13.905	0.029
14	11.048	0.023
15	12.000	0.025

StDev	1.54618
t (n-1, 0.01)	2.624
t value for 99% at n (from Table)	
MDL	4.057

For Arizona groundwater

Sample #	C (ppb)	Abs
1	8.955	0.022
2	9.864	0.024
3	10.318	0.025
4	8.500	0.021
5	8.500	0.021
6	9.409	0.023
7	12.591	0.03
8	10.318	0.025
9	8.045	0.02
10	8.500	0.021
11	10.318	0.025
12	8.500	0.021
13	8.500	0.021
14	13.500	0.032
15	9.864	0.024

StDev	1.57146
t (n-1, 0.01)	2.624
t value for 99% at n (from Table)	
MDL	4.124

APPENDIX B

SUPPLEMENTAL TABLES

Table S1. Raw Water Qualities of Two Water Matrices

Parameters	Model water	Arizona groundwater
Total dissolved Cr (μg/L)	0	7.42$\pm$1.05
Dissolved Cr(VI) (μg/L)	0	6.37$\pm$1.53
Total dissolved Sn (μg/L)	0	11.31 $\pm$4.71
pH	8.47$\pm$0.05	8.25$\pm$0.11
Turbidity	0	4.62$\pm$2.35
Conductivity (μS/m)	446.52$\pm$5.12	1440$\pm$55
DOC concentration (mg/L)	0	1.22$\pm$0.01

Table S2. Observed Rate Constants of 104 µg/L $Cr_2O_7^{2-}$ Reduction with 255, 850, and

1700 µg/L Sn^{2+} at pH = 8.50 ± 0.05

$[Sn^{2+}]_0/[Cr_2O_7^{2-}]_0$	$[Sn^{2+}]$ (**µM**)	log $[Sn^{2+}]$	k_{obs} (**µM^{-2}.s^{-1}**)	log k_{obs}
10.5	5.048	0.703	1.340	0.127
15	7.212	0.875	1.656	0.219
30	14.423	1.176	3.414	0.553

Table S3. Observed Rate Constants of 104 µg/L $Cr_2O_7^{2-}$ Reduction by 1700 µg/L Sn^{2+} at

pH = 7.50±0.05, 8.50±0.05, 9.50±0.05

pH	k_{obs} ($\mu M^{-2}.s^{-1}$)	$\log k_{obs}$
7.5	1.701	0.231
8.5	2.336	0.368
9.5	5.510	0.741

APPENDIX C

SUPPLEMENTAL FIGURES
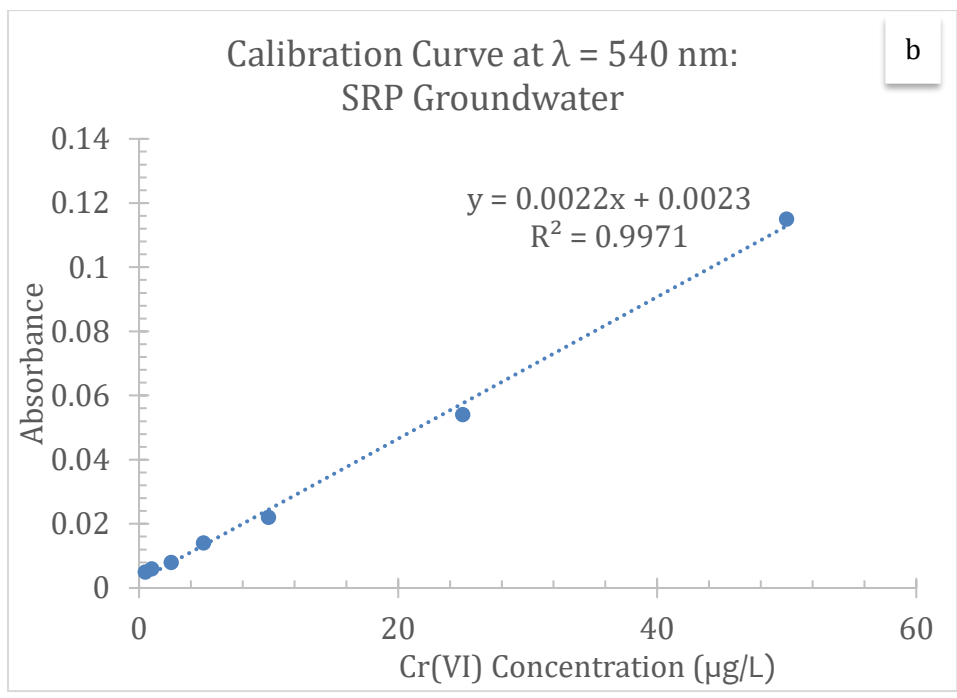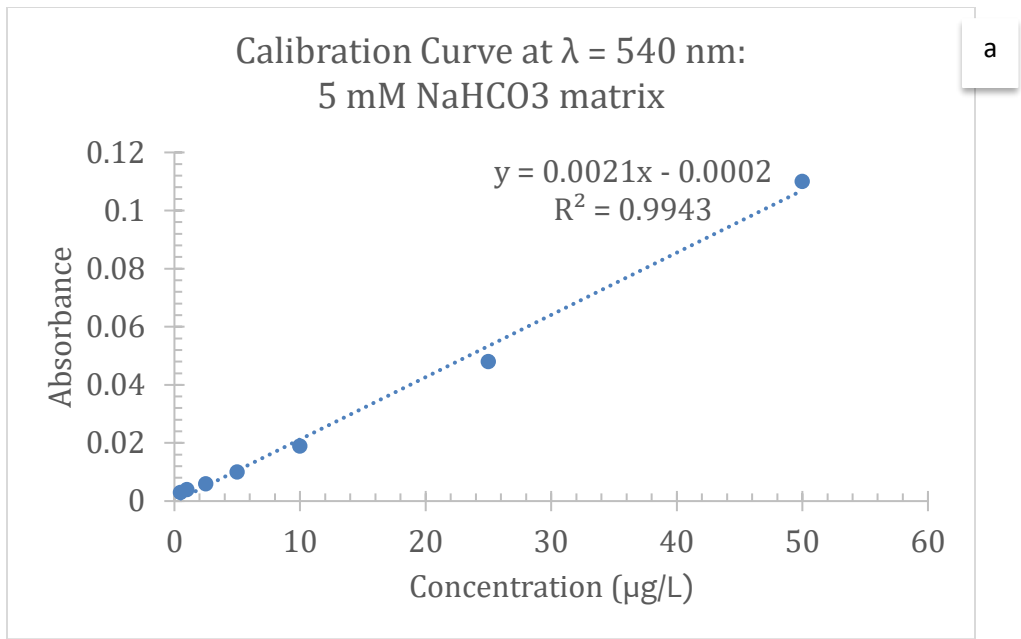
Figure S1. Calibration Curves for Cr(VI) Determination by Colorimetric Method in
a/Buffered Ultrapure Water and Arizona Groundwater
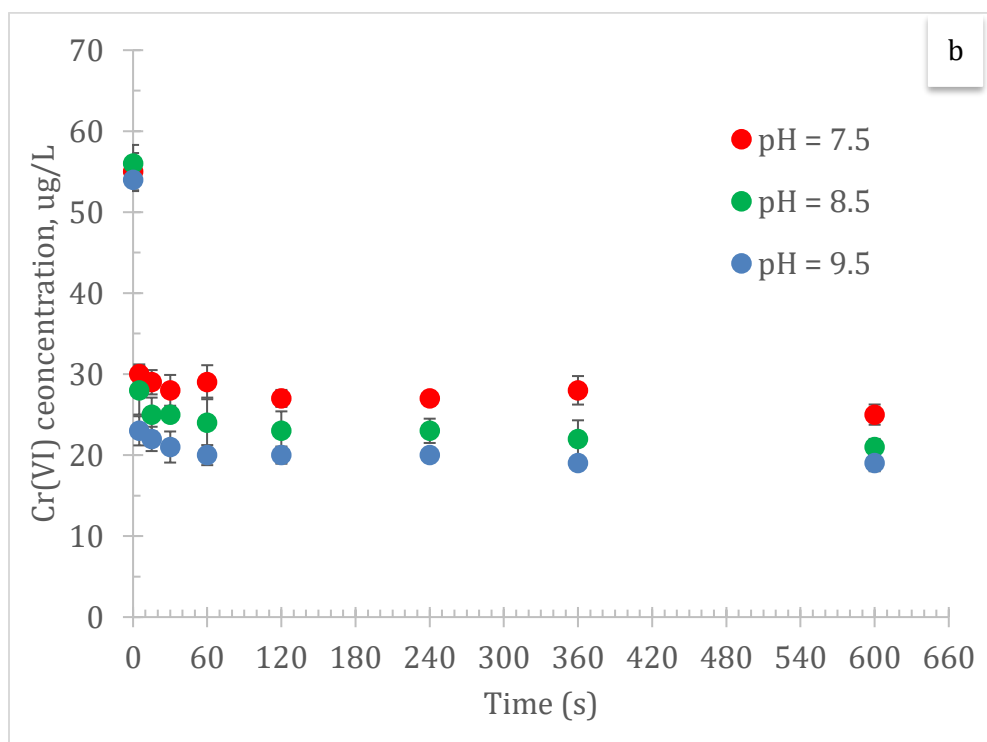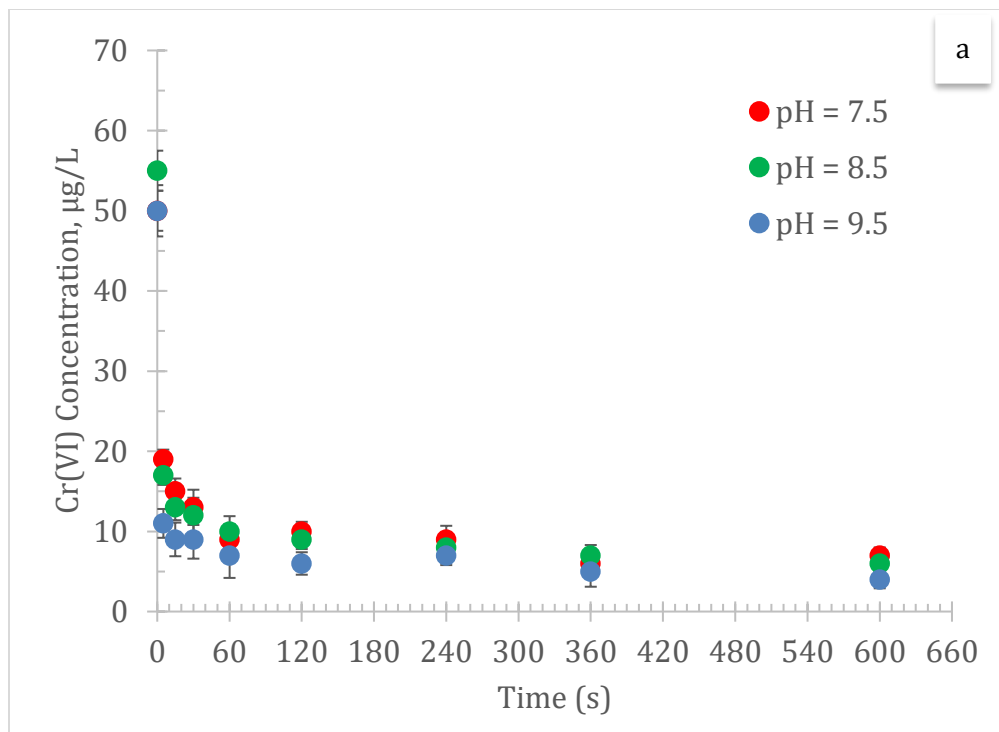
Figure S2. Kinetics of Cr(VI) Reduction by SnCl$_2$ Dosing at a/Stoichiometric and

b/Half-stoichiometric ratio at pH = 7.5, 8.5, 9.5
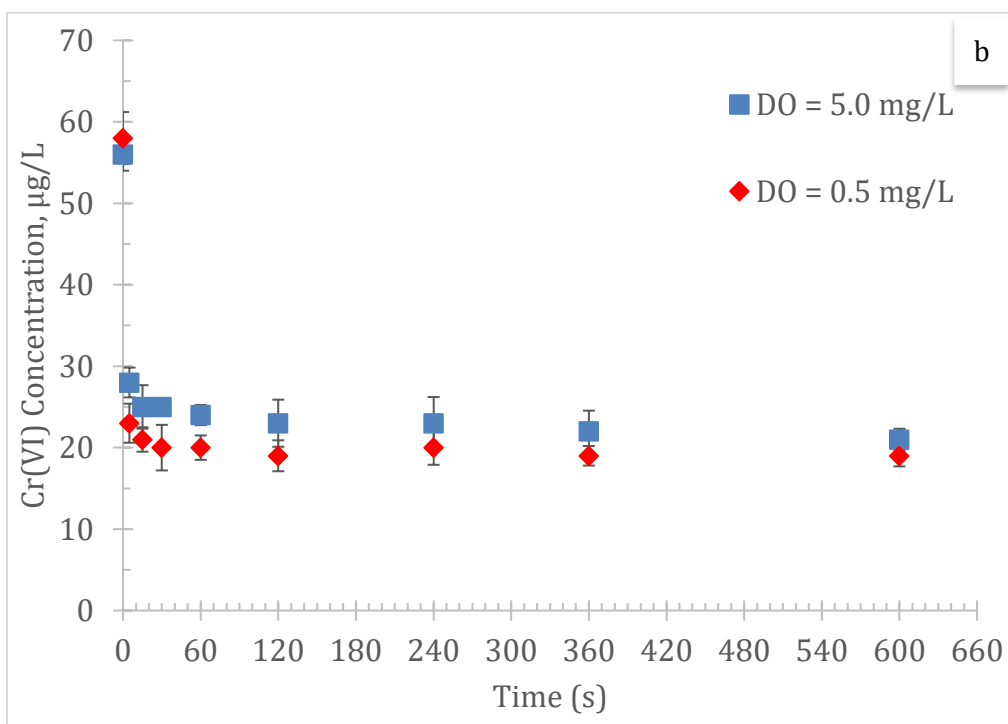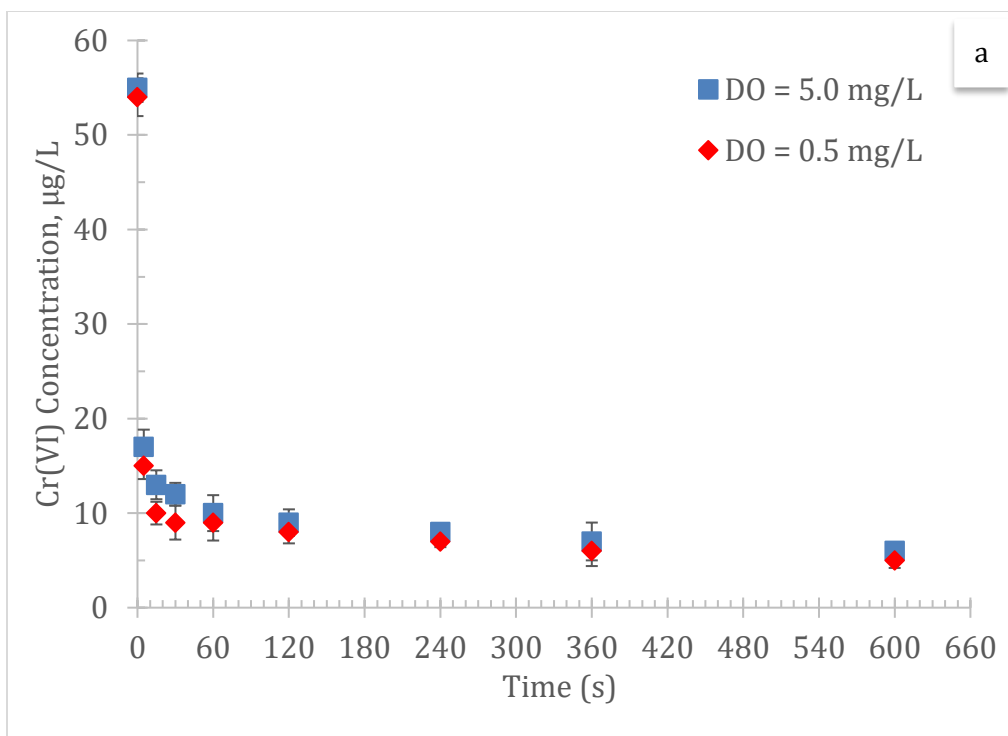
Figure S3. Kinetics of Cr(VI) Reduction by SnCl$_2$ Dosing a/Stoichiometric and

b/Half-stoichiometric Ratio at DO Level = 5.0 and 0.5 mg/L
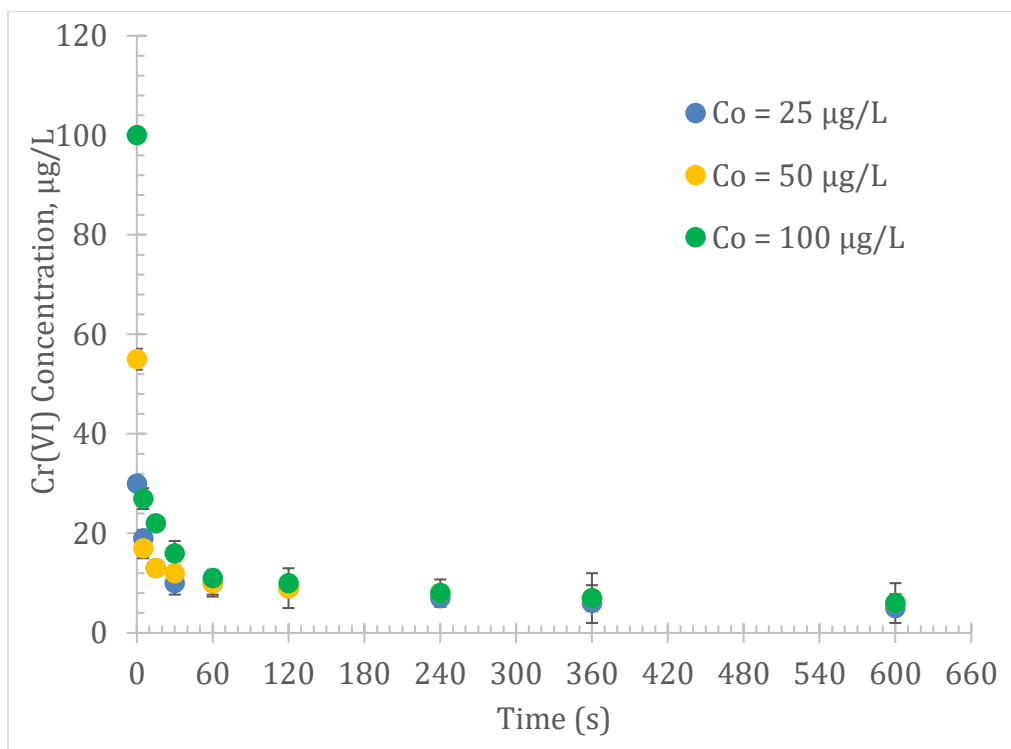
Figure S4. Kinetics of Cr(VI) Reduction by SnCl$_2$ with Initial Cr(VI) Concentrations of

25, 50, 100 µg/L at SnCl$_2$ Stoichiometric Dosing
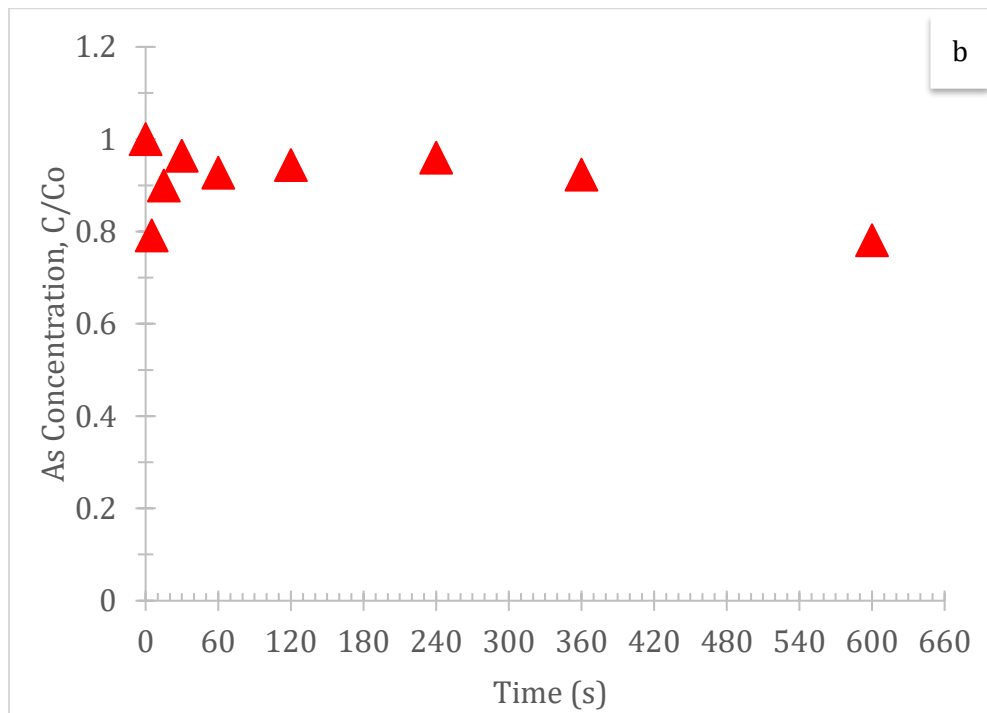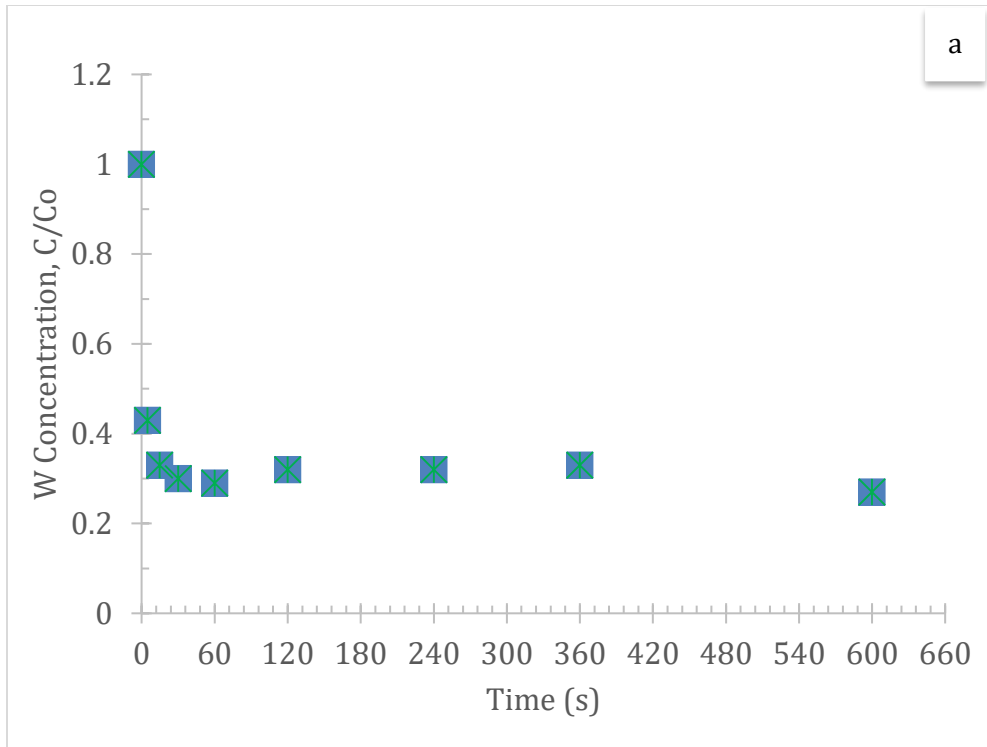
Figure S5. Removal of Total a/Tungstate (W) and b/Arsenic (As) after Adding SnCl$_2$

Stoichiometric Dosage
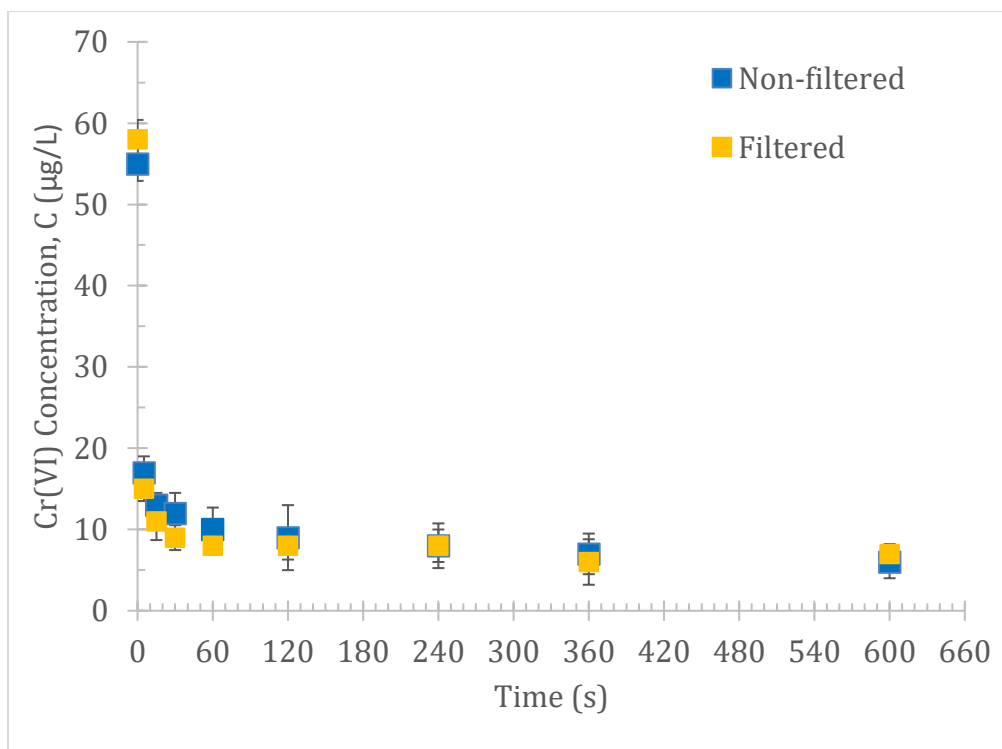
Figure S6. Comparison of Cr(VI) Reduction Kinetics between Filtered and Unfiltered

Samples at Stoichiometric Dosing
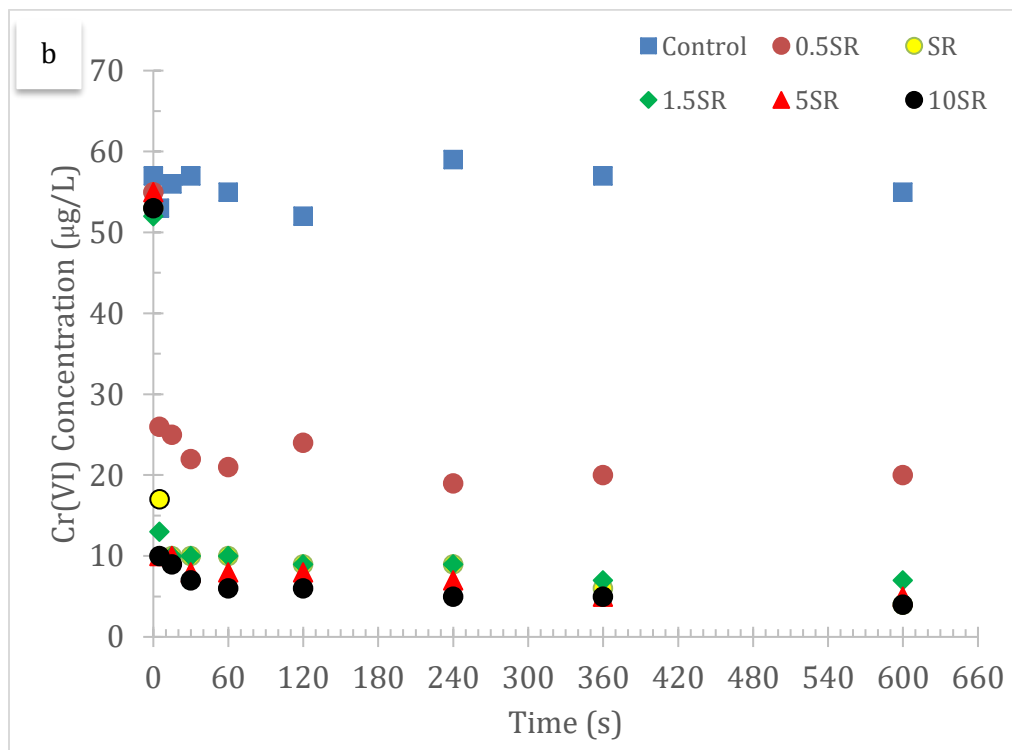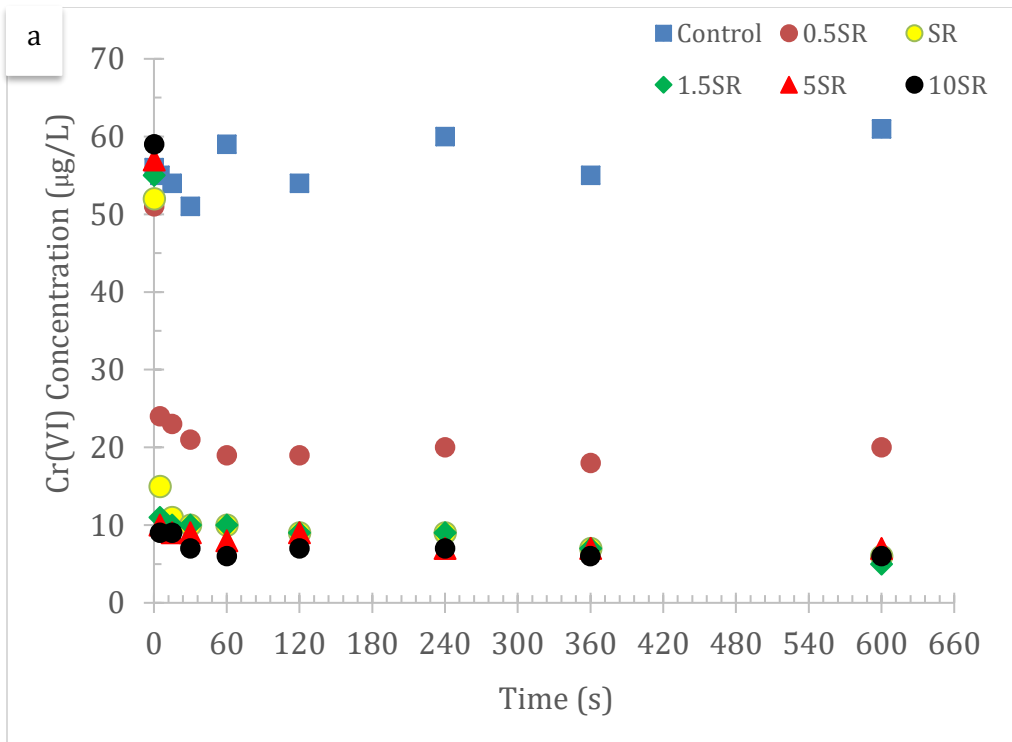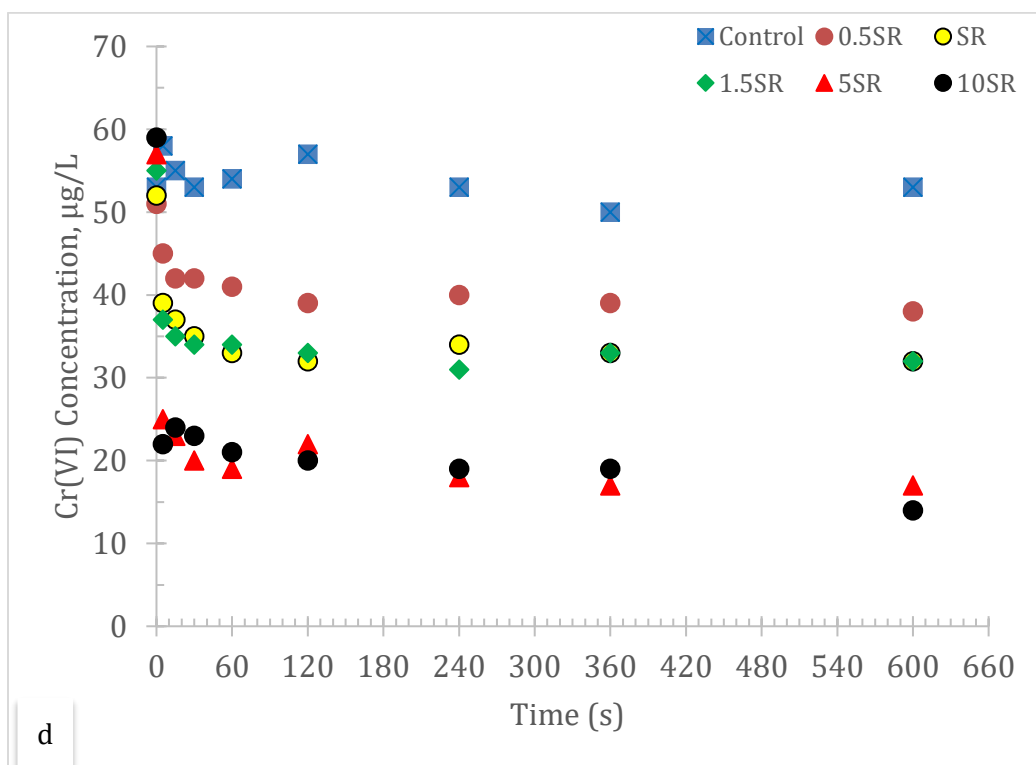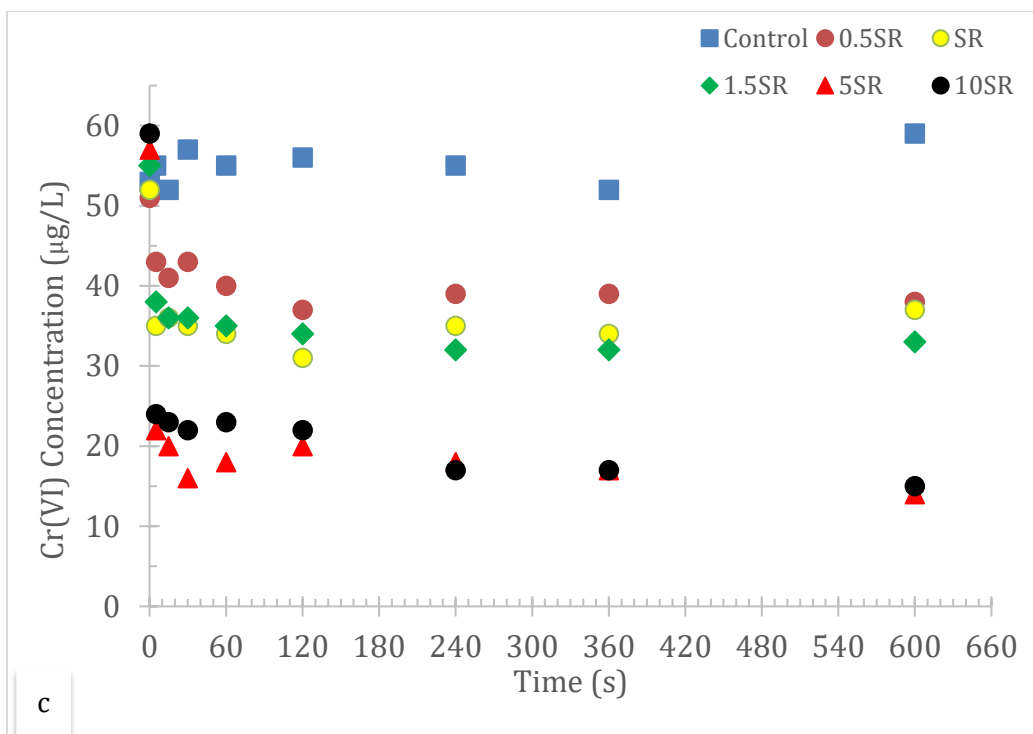
Figure S7. Kinetics of Cr(VI) Reduction by SnCl$_2$ Guard Product a/Experiment 1,

b/Experiment 2, c/Experiment 3, d/Experiment 4
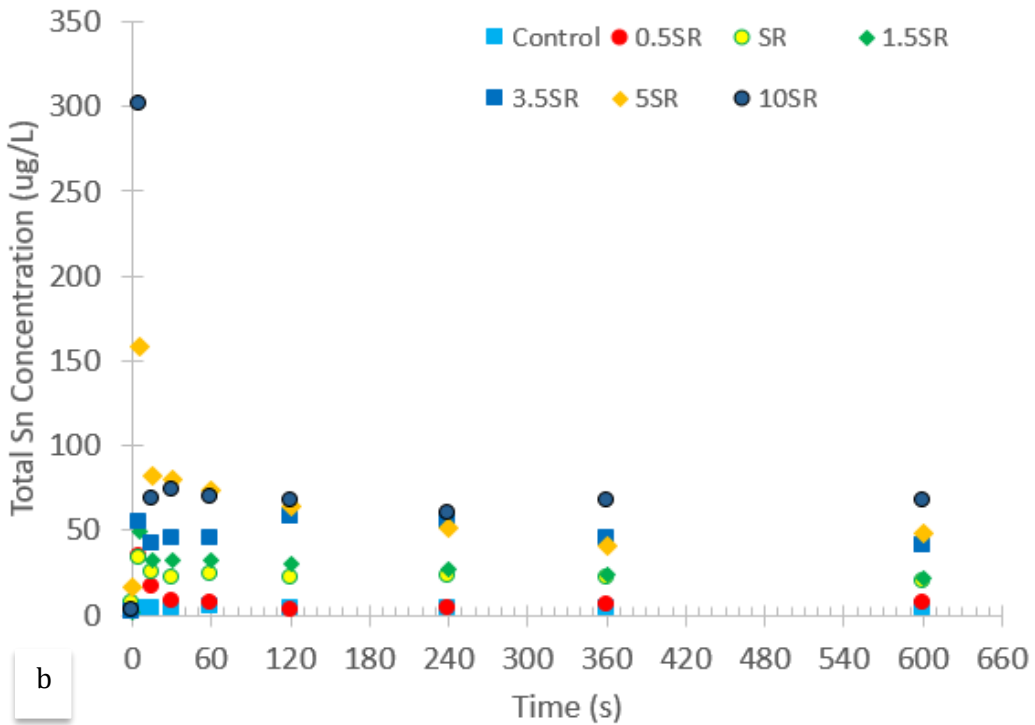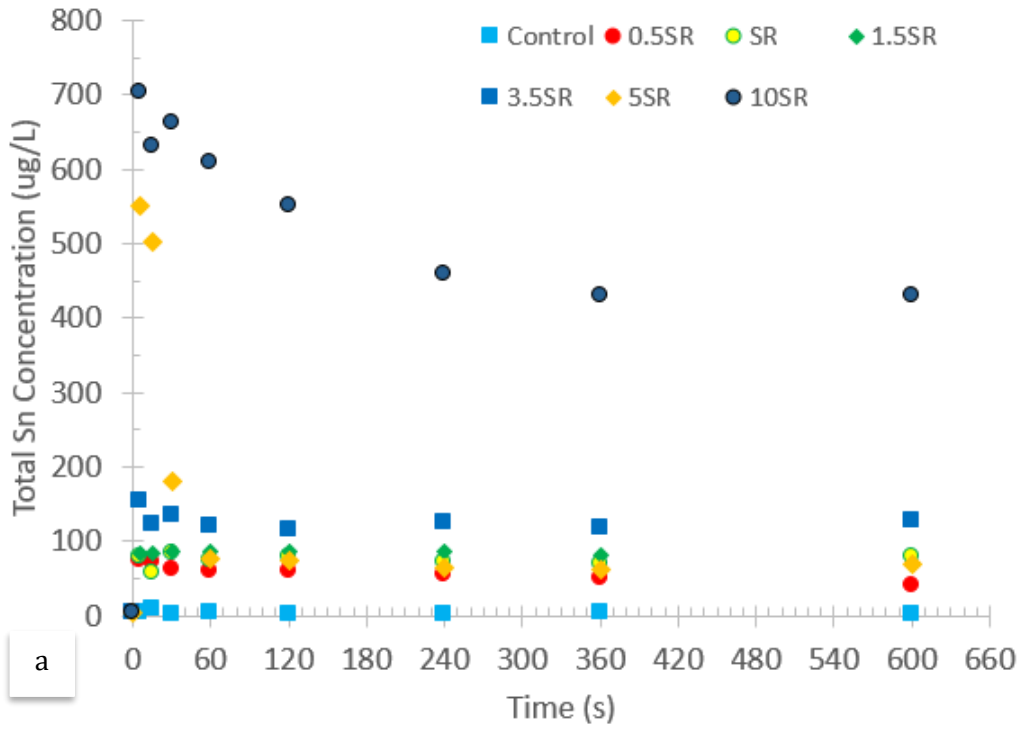
Figure S8. Total Sn Concentration in a/Unfiltered Sample and b/Filtered Sample During

the Reaction with Cr(VI) in Buffered Ultrapure Water

y = 2.679x + 15.04
$R^2 = 0.9794$

a

y = 3.308x + 19.803
$R^2 = 0.9707$

b
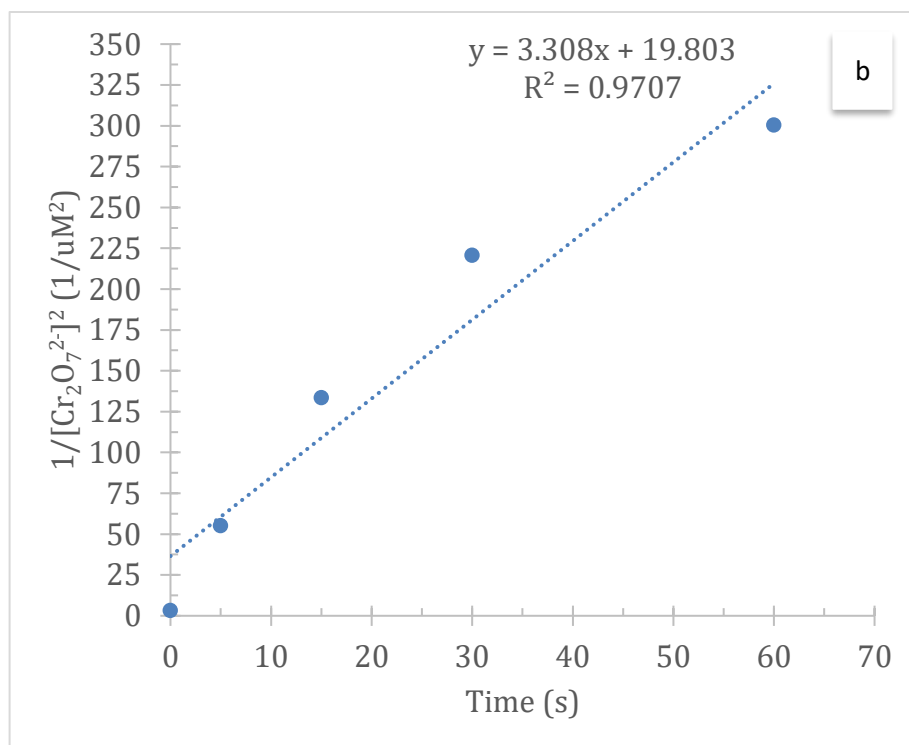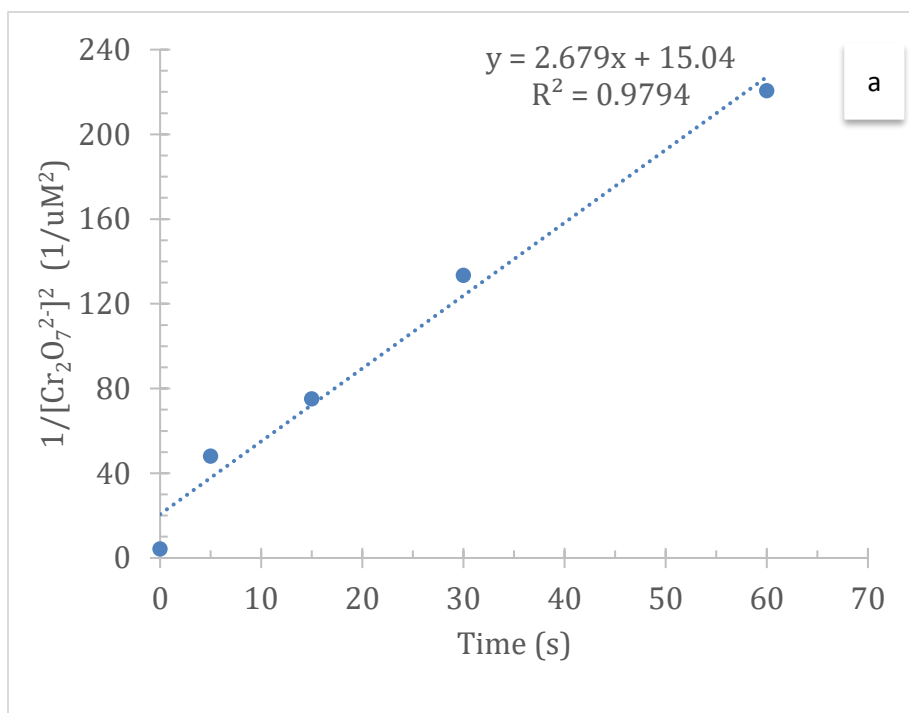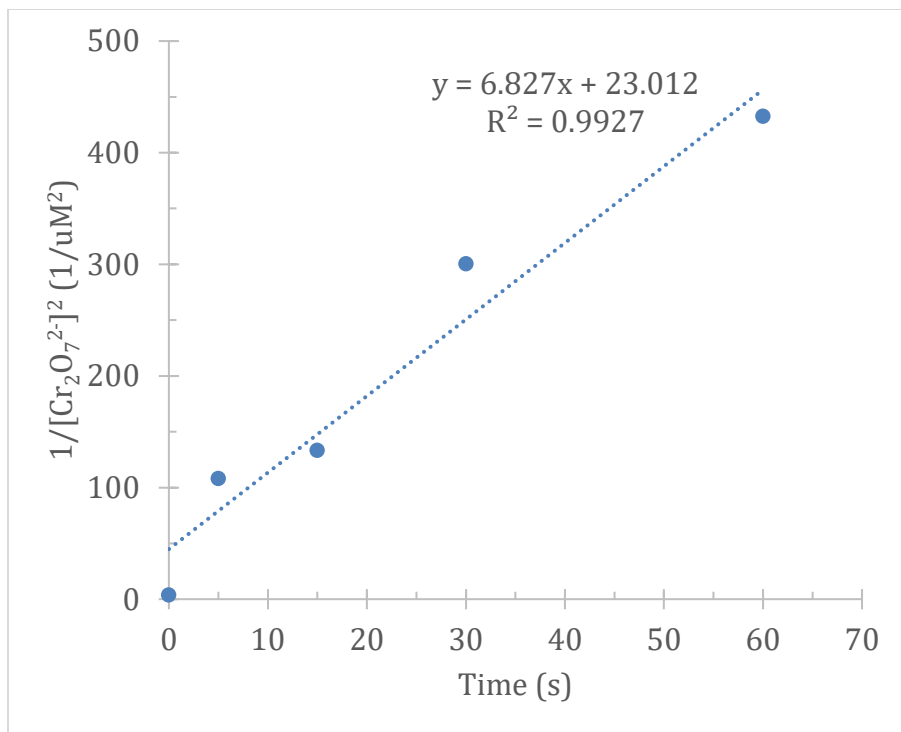
Figure S9. Linear Regression of $1/[Cr_2O_7^{2-}]^2$ Versus Time at Different $[Sn^{2+}]_0/[Cr_2O_7^{2-}]_0$

Ratios of a/10.5, b/15, c/30

$y = 3.4014x + 24.314$
$R^2 = 0.9724$

a

$y = 4.6709x + 44.005$
$R^2 = 0.928$

b

$$y = 11.02x + 45.861$$
$$R^2 = 0.9792$$
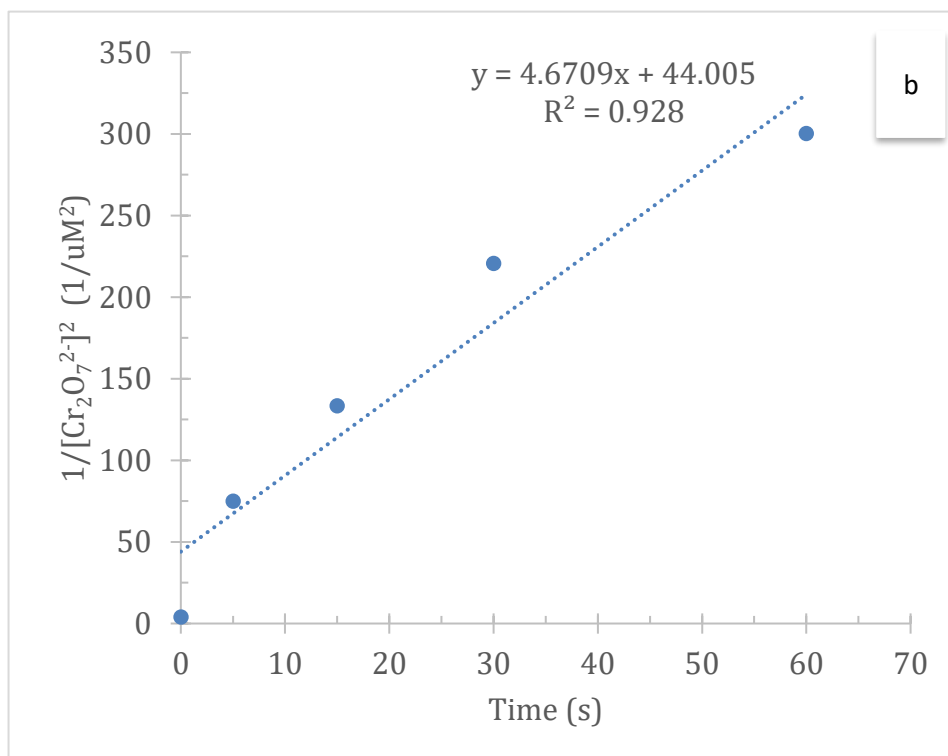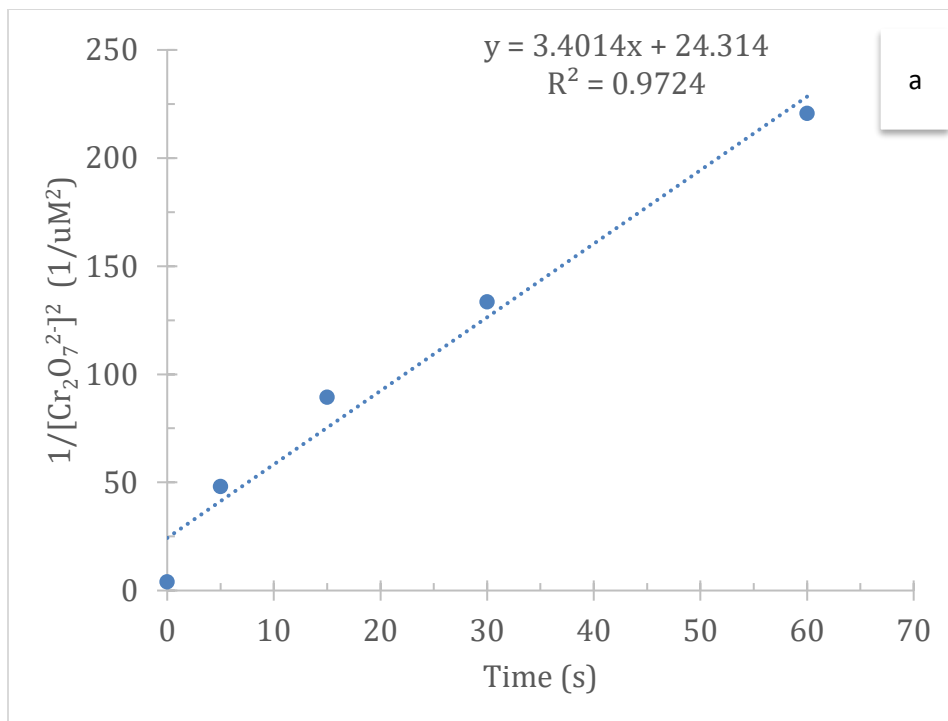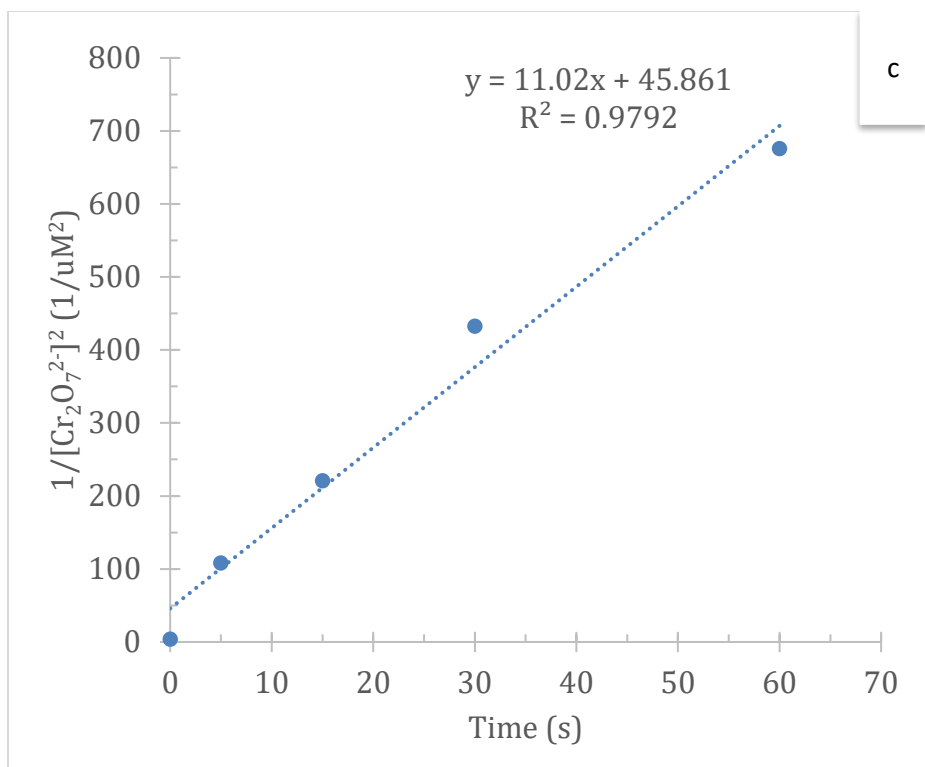
Figure S10. Linear Regression of $1/[Cr_2O_7^{2-}]^2$ Versus Time at Different pH Values: a/7.5,

b/8.5, c/9.5 ($[Sn^{2+}]_0/[Cr_2O_7^{2-}]_0 = 30$)
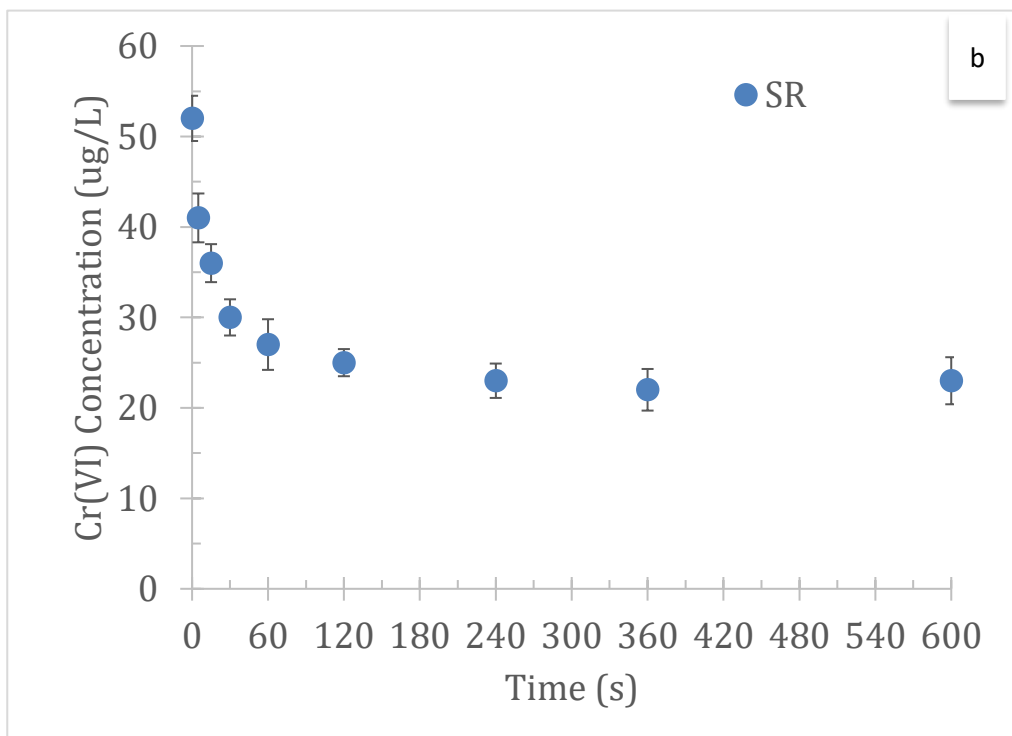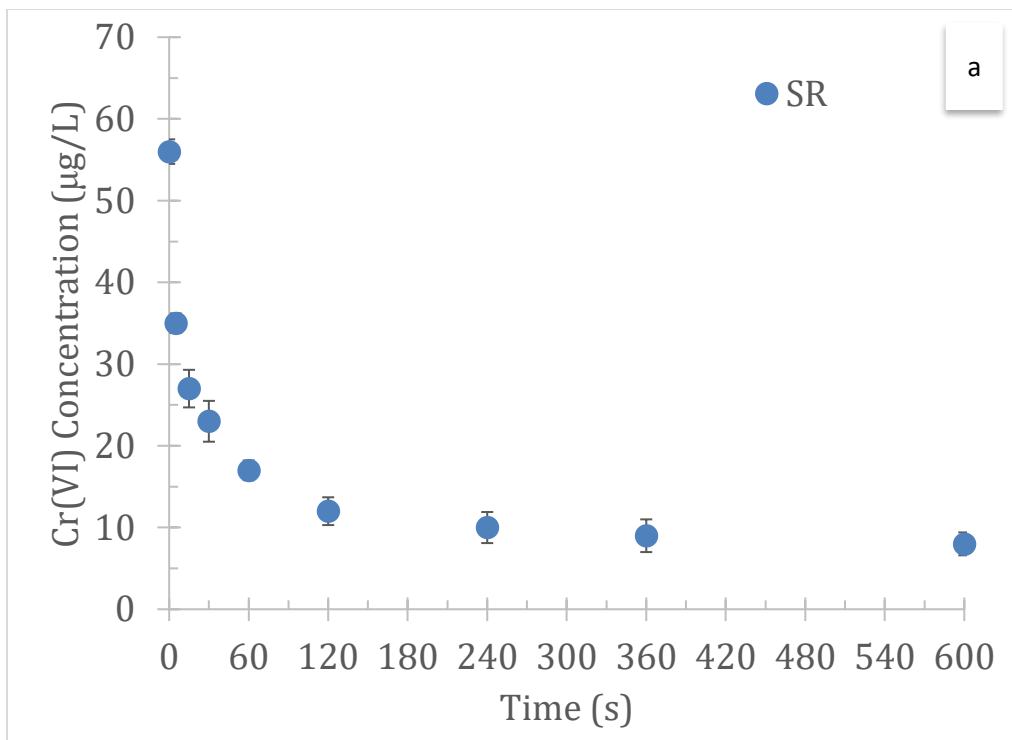
Figure S11. Kinetics of Cr(VI) Reduction by FeSO$_4$ in a/Buffered Ultrapure Water and

b/Arizona Groundwater